AEDC-TR-73-182

cy. 5

MAY 31 1974

# RESONANCE LINE ABSORPTION METHOD FOR DETERMINATION OF NITRIC OXIDE CONCENTRATION


W. K. McGregor and J. D. Few

ARO, Inc.

and

C. D. Litton

The University of Tennessee Space Institute


December 1973

Approved for public release; distribution unlimited.

**ENGINE TEST FACILITY**

**ARNOLD ENGINEERING DEVELOPMENT CENTER**

**AIR FORCE SYSTEMS COMMAND**

**ARNOLD AIR FORCE STATION, TENNESSEE**


Property of U. S. Air Force
AEDC LIBRARY
F40600-74-C-0001

# NOTICES

When U. S. Government drawings specifications, or other data are used for any purpose other than a definitely related Government procurement operation, the Government thereby incurs no responsibility nor any obligation whatsoever, and the fact that the Government may have formulated, furnished, or in any way supplied the said drawings, specifications, or other data, is not to be regarded by implication or otherwise, or in any manner licensing the holder or any other person or corporation, or conveying any rights or permission to manufacture, use, or sell any patented invention that may in any way be related thereto.

Qualified users may obtain copies of this report from the Defense Documentation Center.

References to named commercial products in this report are not to be considered in any sense as an endorsement of the product by the United States Air Force or the Government.

# RESONANCE LINE ABSORPTION METHOD FOR DETERMINATION OF NITRIC OXIDE CONCENTRATION

W. K. McGregor and J. D. Few
ARO, Inc.

and

C. D. Litton
The University of Tennessee Space Institute

Approved for public release; distribution unlimited.

## FOREWORD

The research reported here was conducted at Arnold Engineering Development Center (AEDC), Air Force Systems Command (AFSC), and was carried out under sponsorship of the USAF Aerospace Research Laboratories, Wright-Patterson AFB, Ohio, under Program Element 65802F.

The results of this research program were obtained by ARO, Inc. (a subsidiary of Sverdrup & Parcel and Associates, Inc.), contract operator of AEDC, AFSC, Arnold Air Force Station, Tennessee. The experiments were performed in Propulsion Research Area (R-2E) of the Engine Test Facility (ETF) under ARO Project number RW5211, and the manuscript was submitted for publication on August 16, 1973.

The authors extend acknowledgement to Mr. Bryan L. Seiber, ARO, Inc., Propulsion Wind Tunnel (PWT), and to Dr. Arthur A. Mason, The University of Tennessee Space Institute (UTSI), for helpful discussions which contributed materially to this work, and to Mr. Howard Glassman, who wrote the computer code for simulation of the spectra.

This technical report has been reviewed and is approved.

MARION L. LASTER
Research and Development Division
Directorate of Technology

ROBERT O. DIETZ
Director of Technology

## ABSTRACT

The details of the derivation of working equations for the determination of the concentration of nitric oxide for measurement of the absorption of individual spectral lines lying between 2270 and 2260 Å in the NO (0,0) $\gamma$-band are presented. It is shown experimentally that the derivation is accurate, that published values of oscillator strengths are adequate, and that measurements of number densities with uncertainty no greater than ±20 percent are possible when proper corrections for the relative line widths of source and absorber are made. The density range of use of the (0,0) $\gamma$-band is from about $10^{14}$ to $10^{16}$ $cm^{-3}$ for path lengths usually encountered in combustion system testing (10 to 100 cm). Extension of the range to larger concentrations by use of the (0,1) $\gamma$-band and the application to media having nonuniform concentration and temperature are discussed.

## CONTENTS


| | | Page |
|---|---|---|
| | ABSTRACT | iii |
| | NOMENCLATURE | vii |
| I. | INTRODUCTION | 1 |
| II. | THEORY OF THE METHOD | |
| | 2.1 Description of the Measurement Procedure | 2 |
| | 2.2 Definition of the Absorption Coefficient | 3 |
| | 2.3 Einstein Equation for Radiation | 7 |
| | 2.4 Spectral Line Shape | 9 |
| | 2.5 Equation for the Species Concentration | 12 |
| | 2.6 Expression for the Oscillator Strength | 13 |
| III. | APPLICATION TO THE NO MOLECULE | |
| | 3.1 Energy Levels | 14 |
| | 3.2 Spectral Lines in the $\gamma$-System | 17 |
| | 3.3 Lines Chosen for Absorption Measurements | 21 |
| | 3.4 Oscillator Strengths for the $\gamma$-System | 21 |
| | 3.5 Modification of Spectral Line Absorption Theory for Multiplets | 24 |
| | 3.6 Final Working Equations | 25 |
| IV. | DESCRIPTION OF EXPERIMENT | |
| | 4.1 Apparatus | 26 |
| | 4.2 Performance of NO Radiation Source | 30 |
| | 4.3 Procedure for Absorption Measurements | 30 |
| V. | RESULTS AND DISCUSSION | |
| | 5.1 Results | 32 |
| | 5.2 Discussion of the Method | 35 |
| VI. | CONCLUSIONS | 38 |
| | REFERENCES | 39 |


## ILLUSTRATIONS


Figure

1. Physical Arrangement for Spectral Line Absorption Measurements . . . 3

2. Transmitted Intensity and Absorption Coefficient in an Absorbing Gas
   a. Continuum Intensity Source . . . 4
   b. Narrow Line Source . . . 6

| Figure | | Page |
|---|---|---|
| 3. | Electronic Energy Level Diagram of NO Molecule Indicating the Various Band Systems | 15 |
| 4. | Allowed Transitions for NO $\gamma$-Bands | 18 |
| 5. | Computer-Generated Band Structure for the NO (0,0) $\gamma$-Band | 19 |
| 6. | Computer-Simulated Spectra for the NO (0,0) $\gamma$-Band at a Temperature of 775°K | |
| | a. Spectrometer Slit Width of 0.0 Å | 20 |
| | b. Spectrometer Slit Width of 0.03 Å | 20 |
| 7. | Diagram of Experimental Apparatus | 27 |
| 8. | Diagram of Discharge Tube Used to Produce NO $\gamma$-Band Radiation | 27 |
| 9. | Diagram of Absorption Cell Used to Contain Samples of NO at Known Pressure and Temperature | 28 |
| 10. | Diagram of Data Recording System Used with Spectrometer | 29 |
| 11. | Portion of (0,0) NO $\gamma$-Band Used for Narrow Line Absorption Measurements | |
| | a. Computer-Simulated Spectra, Slit Width of 0.03 Å | 31 |
| | b. Spectrum from Source, Slit Width of 0.03 Å | 31 |
| | c. Rotational Line Location | 31 |
| 12. | Experimental Data from Absorption Measurements of NO $\gamma$-Band Radiation Passing through a Low-Pressure Absorption Tube Containing NO | |
| | a. Run Number 1 | 32 |
| | b. Run Number 2 | 33 |
| 13. | Theoretical and Experimental Transmission of Several NO (0,0) $\gamma$-Band Lines through NO Gas at Various Pressures | |
| | a. $Q_{22}(25/2) + R_{12}(25/2)$, line 4 | 34 |
| | b. $Q_{22}(23/2) + R_{12}(23/2)$, line 5 | 34 |
| | c. $P_{22}(35/2) + Q_{12}(35/2)$, line 6 | 34 |
| | d. $R_{22}(13/2)$, line X | 34 |
| | e. $Q_{22}(21/2) + R_{12}(21/2)$, line 7 | 34 |
| | f. $Q_{22}(15/2) + R_{12}(15/2)$, line 11 | 34 |
| | g. $Q_{22}(13/2) + R_{12}(13/2)$, line 12 | 34 |
| | h. $Q_{22}(9/2) + R_{12}(9/2)$, line 15 | 34 |

Figure | Page

14. Boltzmann Plot of Rotational Line Transmission for Determination of Rotational Temperature . . . . . 35

TABLES

I. Molecular Constants Used to Calculate Spectral Line Wavelengths and Intensities for the NO $\gamma$-Bands . . . . 17

II. Line Identification and Data for Spectral Peaks Useful for NO Concentration Measurements . . . . . 21

III. Franck-Condon Factors for the $\gamma$-Bands of NO . . . . . 22

IV. Hönl-London Factors for $^2\Sigma \rightarrow {}^2\pi$ Transitions Intermediate between Hund's Cases (a) and (b) . . . . . 23

## APPENDIXES

I. DESCRIPTION OF METHOD FOR CONVERSION OF MEASURED LINE TRANSMISSION TO LINE CENTER TRANSMISSION FOR NON-NARROW LINE SOURCES . . . 41

II. DESCRIPTION OF COMPUTER SIMULATION OF BAND SPECTRA . . . . . 44

## NOMENCLATURE

| | |
|---|---|
| $\alpha$ | Absorptivity of radiation by a medium |
| $\nu$ | Frequency, $cm^{-1}$ |
| $I^o$ | Incident radiation intensity, arbitrary but consistent units |
| $I_m$ | Measured radiation intensity, arbitrary but consistent units |
| $t_\nu$ | Transmissivity of radiation through a medium at frequency, $\nu$ |
| $\Delta\nu$ | Frequency interval, $cm^{-1}$ |
| $k_\nu$ | Absorption coefficient at frequency, $\nu$, $cm^{-1}$ |

| | |
|---|---|
| $\ell$ | Path length, cm |
| $I_\nu$ | Radiation intensity at frequency, $\nu$, arbitrary units |
| $I_\nu^o$ | Incident radiation intensity at frequency, $\nu$, arbitrary units |
| $k_{\nu_o}$ | Absorption coefficient at line center frequency, $\nu_o$, $cm^{-1}$ |
| $I_m^o$ | Measured source intensity, arbitrary units |
| L | Total path length, cm |
| $I_{\nu_o}$ | Radiation intensity at line center frequency, $\nu_o$, arbitrary units |
| $t_m$ | Measured transmissivity of radiation through a medium |
| $J''$ | Rotational angular momentum quantum number of lower state |
| $J'$ | Rotational angular momentum quantum number of upper state |
| $A_{J'J''}$ | Probability of a spontaneous radiating transition from quantum state $J'$ to quantum state $J''$, $sec^{-1}$ |
| $N_{J'}, N_{J''}$ | Number of molecules in quantum state $J'$ and quantum state $J''$, respectively, molecules/$cm^3$ |
| $B_{J'J''}$ | Probability per unit radiation intensity at frequency $\nu$ of an induced radiating transition from quantum state $J'$ to quantum state $J''$, $sec^{-1}$/intensity unit |
| $B_{J''J'}$ | Probability per unit radiation intensity at frequency $\nu$ of an induced absorbing transition from quantum state $J''$ to quantum state $J'$, $sec^{-1}$/intensity unit |
| h | Planck's constant, $6.625 \times 10^{-27}$ erg sec |
| c | Velocity of light, $3 \times 10^{10}$ cm/sec |
| $g_{J''}, g_{J'}$ | Statistical weights of the lower and upper quantum states, respectively |
| $N_{\nu_{J''}}, N_{\nu_{J'}}$ | Number of molecules capable of absorbing a photon of frequency $\nu$ or emitting a photon of frequency $\nu$, respectively, molecules/$cm^3$ |
| $E_{J''}, E_{J'}$ | Potential energy of the lower $J''$ quantum state and the upper $J'$ quantum state, respectively, $cm^{-1}$ |
| $\kappa$ | Boltzmann's constant, 0.6952 $cm^{-1}$/°K |

| | |
|---|---|
| $T$ | Temperature, °K |
| $e$ | Charge on the electron, $4.803 \times 10^{-10}$ esu |
| $f_{J'J''}$ | Oscillator strength for a spectral line corresponding to a transition from the $J'$ to the $J''$ quantum state |
| $\Delta\nu_D$ | Half-width of an emission or absorption line due to Doppler broadening, $cm^{-1}$ |
| $M$ | Mass of molecule, gm |
| $t_{\nu_o}$ | Transmission at line center frequency, $\nu_o$ |
| $y$ | Distance from axis of cylinder, cm |
| $r$ | Radius of cylinder, at any value y, cm |
| $R$ | Radius of cylinder, cm |
| $\mathcal{T}_e$ | Term energy of an electronic state, $cm^{-1}$ |
| $G(v)$ | Vibrational energy of the vth quantum state, $cm^{-1}$ |
| $F(J'')$ | Rotational energy of the $J''$th quantum state, $cm^{-1}$ |
| $S$ | Electron spin angular momentum quantum number |
| $N_o$ | Total number density of absorbing species, molecules/$cm^3$ |
| $Q_e, Q_v, Q_R$ | Electronic, vibrational, and rotational partition functions, respectively |
| $f_{J'J''}$ | Oscillator strength of a single transition from the $J'$ rotational state of the upper electronic-vibrational level to the $J''$ rotational state of the lower electronic-vibrational level |
| $f_{v'v''}$ | Oscillator strength for all rotational transitions from the $v'$ vibrational level to the $v''$ vibrational level |
| $f_{e\ell}$ | Electronic oscillator strength |
| $q_{v'v''}$ | Vibrational overlap integral, or Franck-Condon factor |
| $\lambda_{v'v''}$ | Wavelength at the bandhead of the $(v',v'')$ band, cm |
| $\lambda_{J'J''}$ | Wavelength of a particular $(J'J'')$ line in the $(v', v'')$ band, cm |
| $\delta_{J'J''}$ | Rotational line strength or Hönl-London factor |
| $\omega_e$ | First vibrational constant, $cm^{-1}$ |
| $\omega_e x_e$ | Second vibrational constant, $cm^{-1}$ |

| | |
|---|---|
| $\omega_e y_e$ | Third vibrational constant, $cm^{-1}$ |
| K | Rotational angular momentum quantum number |
| $B_v$ | First rotational constant, $cm^{-1}$ |
| $D_v$ | Second rotational constant, $cm^{-1}$ |
| $\alpha_e$ | Third rotational constant, $cm^{-1}$ |
| $\beta_e$ | Fourth rotational constant, $cm^{-1}$ |
| $F_n(J)$ | Rotational energy of the Jth quantum state, n = 1, $F_1(J - 1/2)$ and n = 2, $F_2(J + 1/2)$, $cm^{-1}$ |
| u | Function used in Hill and van Fleck formula |
| $Y_v$ | Constant used in Hill and van Fleck formula |
| A | Uncoupling constant for states intermediate between Hund's coupling cases (a) and (b) |
| $\Gamma$ | Splitting constant for states in Hund's coupling case (b) |
| U | Function used in Hönl-London factor expressions for states intermediate between Hund's cases (a) and (b) |
| C | Defined constant used in final equation relating number density of molecules to the measured absorption coefficient |
| a | Ratio of the line width of the radiation source to the line width of the absorbing gas |
| W | Defined function of frequency |
| $\lambda$ | Wavelength, cm |

# SECTION I
# INTRODUCTION

A large effort is currently being put forth to measure the contribution to atmospheric pollution of nitric oxide (NO) for automobile and jet engine exhausts. Techniques used to measure NO concentrations have generally been hindered by (1) the small concentrations which are encountered in pollution sources (on the order of 100 parts per million), and (2) the tendency of NO to chemically combine with other compounds in sample cells and hence reduce the actual concentration in the sample measured. No completely satisfactory method has been developed to measure NO concentrations. Reported herein are the results of an investigation of the feasibility of a nonsampling, in situ, ultraviolet absorption method to measure NO concentrations.

The specific purpose of the work reported herein was to develope a technique to determine concentrations of NO from measurement of the absorption of spectral lines lying in the ultraviolet $\gamma$-bands of NO. The narrow line absorption technique has been in use for many years but application to the NO molecule has not been made, principally because of the inability of ordinary spectrometric equipment to completely resolve the rotational lines in the NO $\gamma$-bands. A lucid explanation of the spectral line absorption technique is contained in the book by Mitchel and Zemansky (Ref. 1) but certain adjustments must be made in order to apply the technique to the NO molecule. The development of the theory of absorption of spectral lines will be systematically made in this report for the sake of clarity, although portions of the treatment appear throughout the literature. Other research programs at AEDC (Refs. 2 and 3) have made use of the narrow line absorption method for determination of hydroxyl (OH) concentrations in flames, but the treatment of the equations for OH is not quite the same as for NO because of the different molecular structure and line broadening properties. Tabulations of the structural properties of the NO molecule are also scattered in the literature, and these data will also be assembled in a systematic manner in this report. Finally, a numerical working equation for determination of NO concentration from measured spectral line transmission will be developed.

In the experimental work, a high-intensity, narrow-line source of NO radiation was developed. Parallel light emanating from the source was passed through a cylindrical absorption cell containing NO at a known partial pressure. The length of the absorption cell was

accurately known, and the diameter of the beam of parallel light passing through the cell was smaller than the diameter of the absorption cell. The concentration of NO as determined from measurements of the temperature and pressure in the absorption cell was compared with the results of the absorption measurement. The results of the comparison were satisfactory, considering the uncertainties in the theory and the measurements. Finally, some implied conclusions about the method, the development of the theory, and applications are discussed.

# SECTION II
# THEORY OF THE METHOD

## 2.1 DESCRIPTION OF THE MEASUREMENT PROCEDURE

The basic principle upon which the measurement technique being described here exists is that a beam of light is absorbed by the gas at some determinable wavelength, and that the magnitude of the absorption is uniquely related to the concentration and temperature of the absorbing species along the path length. The measurement required is the absorptivity

$$\alpha_\nu = [(I^o - I_m)/I^o]_\nu$$

or transmissivity

$$t_\nu = [I_m/I^o]_\nu$$

within a given wave number interval ($\Delta\nu$) where $I^o$ is the incident intensity and $I_m$ is the transmitted intensity as illustrated in Fig. 1. The problem is to relate this measurement to the properties (concentration of absorbing species, temperature, and pressure) of the absorbing medium. This section is devoted to a systematic derivation of the relationship between the measured transmission and the concentration and temperature of the NO molecule and the pressure of the absorbing medium.

The (0,0) band of the ultraviolet resonance $\gamma$-system of NO was chosen for the measurements. The first band-head of the (0,0) band is at 2269.4 Å. NO has an infrared absorption spectrum at about 5.2 microns, but this region of the spectrum is cluttered with band systems of other molecules such as CO and several minor components of

combustion gases. The 2269 Å region does not suffer from overlapping of other bands.

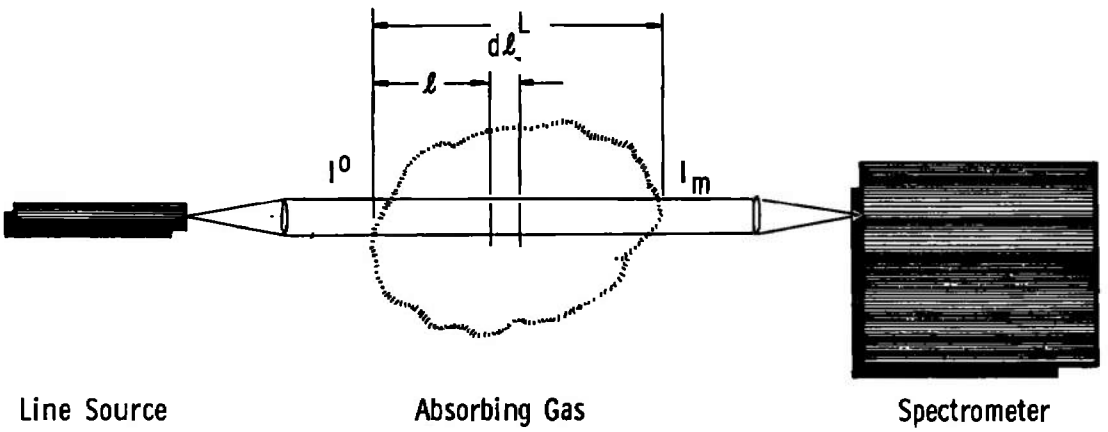


**Fig. 1 Physical Arrangement for Spectral Line Absorption Measurements**

## 2.2 DEFINITION OF THE ABSORPTION COEFFICIENT

If radiation from a continuum source is directed through a gas as shown in Fig. 1, the transmitted beam will suffer absorption at selected wave numbers appropriate to the gas species. The absorption coefficient ($k_\nu$) of the gas at some appropriate wave number ($\nu$) is defined by the equation (Ref. 1):

$$\frac{dI_\nu}{d\ell} = -k_\nu I_\nu \tag{1}$$

where $I_\nu$ is the intensity of a beam of light of wave number ($\nu$) at a distance ($\ell$) into the gas, and $dI_\nu$ is the decrease in intensity after passing through a thickness ($d\ell$) of the gas. If the gas has uniform properties, then $k_\nu$ will be independent of the position and Eq. (1) may be integrated to give

$$\frac{I_\nu}{I_\nu^o} = \exp(-k_\nu L) \tag{2}$$

where $I_\nu^o$ is the incident intensity at wave number ($\nu$) at the entrance to the absorbing layer of thickness (L). If the properties are not uniform,

then

$$\frac{I_\nu}{I_\nu^o} = \exp\left(-\int k_\nu d\ell\right) \tag{3}$$

For a real gas, the absorption coefficient of an absorption line is a function of the frequency or wave number; that is, the envelope of the transmission $((I/I^o)_\nu)$ and the absorption coefficient $(k_\nu)$ of a continuum source will have the approximate shapes shown in Fig. 2a. The total width of the absorption coefficient curve at the frequency where $k_\nu$ has fallen to one-half of $k_{\nu_o}$, its maximum value, is called the half-width of the absorption line and is denoted as $\Delta\nu$. In general, the absorption coefficient of a gas is given by an expression involving a function of $\nu$ and a definite value of $k_{\nu_o}$ and $\Delta\nu$, both of which are functions of the local gas pressure and temperature.

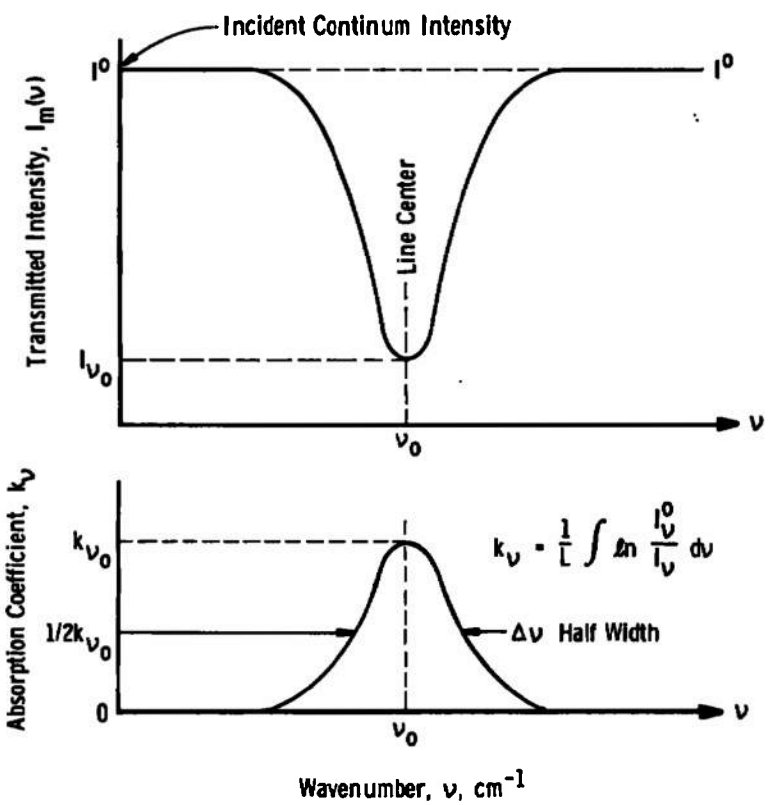


**a. Continuum Intensity Source**

**Fig. 2 Transmitted Intensity and Absorption Coefficient in an Absorbing Gas**

In most practical cases in the ultraviolet portion of the spectrum, $\Delta\nu$ is much smaller than the band-pass of the instruments that must be used, so that it is the integral over frequency that is measured:

$$I_m = \int_0^\infty I_\nu^o \exp(-k_\nu L) d\nu \tag{4}$$

If the source is a continuum, then $I_{\nu_o}$ is a constant and may be removed from the integral:

$$I_m = I^o \int_{2\Delta\nu} \exp(-k_\nu L) d\nu \tag{5}$$

and the transmission ($t_m = (I_m/I^o)$) is a measure of the absorption integral.

Now, suppose the source is not a continuum but a line at the same frequency as the absorption line but much narrower, as illustrated in Fig. 2b. Then, absorption takes place only over the extent of the incident radiation:

$$I_m = \int_{2\Delta\nu} I_\nu^o \exp(-k_\nu L) d\nu \tag{6}$$

But now $k_\nu$ is just the absorption at line center ($k_{\nu_o}$) and is constant over the integral:

$$I_m = \exp(-k_{\nu_o} L) \int_{2\Delta\nu} I_\nu^o d\nu = I_{\nu_o}^o \exp(-k_{\nu_o} L) \tag{7}$$

This latter expression is much simpler than Eq. (5) and does not depend on the line shape. This is the essence of the narrow line absorption technique. Furthermore, the measured transmission ($t_m = I_m/I_{\nu_o}^o$) is a sensitive function of $k_{\nu_o}$.

Suppose that the incident line is not much narrower than the absorption line. The measured transmission is not now a simple function of the absorption coefficient as in the cases defined by Eqs. (5) and (7). Rather, the relationship becomes

$$t_m = \frac{I_m}{I_m^o} = \frac{\int I_\nu d\nu}{\int I_\nu^o d\nu} = \frac{\int I_\nu^o \exp(-k_\nu L) d\nu}{\int I_\nu^o d\nu} \tag{8}$$

involving the details of the incident source variation with wave number and the absorption line shape. This is the more general line absorption problem and, although much more difficult because of the integration problems, is still much more sensitive to a change in $k_\nu$ than the continuum expression (Eq. (5)).

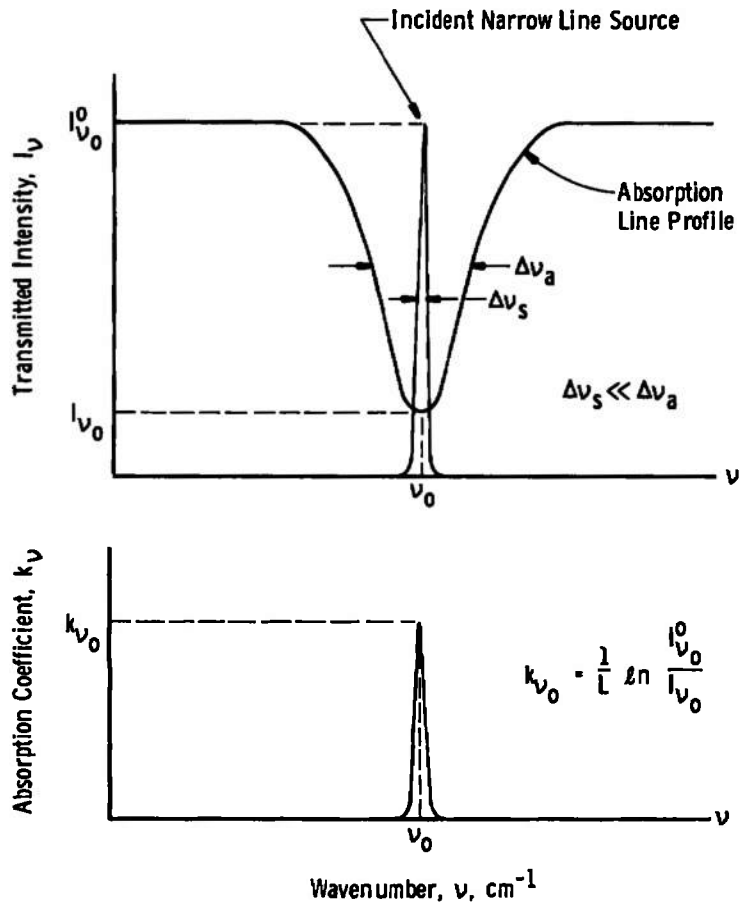


**b. Narrow Line Source**
**Fig. 2 Concluded**

The problem is, then, to determine means by which the measured transmission may be related to the properties of the gas, which are expressible through $\int k_\nu d\nu$. In the following sections, the relationship between $\int k_\nu d\nu$ and the gas temperature, pressure, and concentration of the absorbing species will be developed, and by examination of the details of the function $(k_\nu)$ means will be found to extract $\int k_\nu \, d\nu$ from the measured transmission.

## 2.3 EINSTEIN EQUATION FOR RADIATION

First, consider the situation in which an enclosure contains isotropic radiation of wave number between $\nu$ and $\nu + d\nu$, intensity $I_\nu$, and molecules capable of being raised by absorption of the radiation from the rotational state $J''$ of one electronic-vibrational level to the state $J'$ of some higher electronic-vibrational level. The Einstein radiation law relates the rate of photon production from a unit volume of gas for a given transition, to the properties of the gas (Ref. 1); that is, the rate of photon production is equal to

$$A_{J'J''}N_{J'} + B_{J'J''}\frac{I_\nu}{4\pi}N_{J'} - B_{J''J'}\frac{I_\nu}{4\pi}N_{J''} \tag{9}$$

where the Einstein transition probabilities are defined by Milne as described in Ref. 1 in terms of intensity as follows:

1. $B_{J''J'}I_\nu$ = probability per second that the molecule in state $J''$ exposed to isotropic radiation of wave number between $\nu$ and $\nu + d\nu$ and intensity, $I_\nu$, will absorb a quantum $hc\nu$ and pass to the state $J'$. (h is Planck's constant and c is the velocity of light.)

2. $A_{J'J''}$ = probability per second that the molecule in state $J'$ will spontaneously emit a quantum $hc\nu$ and pass to the state $J''$.

3. $B_{J'J''}I_\nu$ = probability per second that the molecule will undergo the transition from $J'$ to $J''$ when it is exposed to isotropic radiation of wave number between $\nu$ and $\nu + d\nu$ and intensity, $I_\nu$, and emit a quantum $hc\nu$.

The Einstein transition probabilities as used in Eq. (9) are related by the following equations (Ref. 1):

$$\frac{A_{J'J''}}{B_{J''J'}} = 2hc\nu^3\frac{g_{J''}}{g_{J'}} \tag{10}$$

$$\frac{B_{J'J''}}{B_{J''J'}} = \frac{g_{J''}}{g_{J'}} \tag{11}$$

where $g_{J''}$ and $g_{J'}$ are the statistical weights of the lower and upper excited states, respectively.

Consider a parallel beam of light of wave number between $\nu$ and $\nu + d\nu$ and traveling in the positive direction through a layer of molecules bounded by the planes at $\ell$ and $\ell + d\ell$ (Fig. 1). Suppose there are $N_{J''}$ molecules per cubic centimeter in the $J''$ state of which $\delta N_{\nu J''}$ are capable of absorbing in the range between $\nu$ and $\nu + \delta\nu$, and $N_{J'}$ excited molecules per cubic centimeter in the $J'$ state of which $\delta N_{\nu J'}$ are capable of emitting in this wave number interval. Assuming that the incident intensity is much greater than the spontaneous emission, the first term on the right of Eq. (9) can be neglected and the decrease in intensity of the incident beam along the path is given by

$$-d[I_\nu \delta_\nu] = \delta N_{\nu J''} h\nu B_{J''J'} \frac{I_\nu}{4\pi} d\ell - \delta N_{\nu J'} h\nu B_{J'J''} \frac{I_\nu}{4\pi} d\ell \tag{12}$$

where $I_\nu / 4\pi$ is the intensity of the equivalent isotropic radiation for which $B_{J''J'}$ and $B_{J'J''}$ are defined. Rewriting Eq. (12) gives

$$-\frac{1}{I_\nu} \frac{dI_\nu}{d\ell} \delta\nu = \frac{h\nu}{4\pi} (B_{J''J'} \delta N_{\nu J''} - B_{J'J''} \delta N_{\nu J'}) \tag{13}$$

By recognizing that the left hand side of the equation is $k_\nu \delta\nu$ with $k_\nu$ as defined by Eq. (1), Eq. (13) becomes

$$k_\nu \delta\nu = \frac{h\nu}{4\pi} (B_{J''J'} \delta N_{\nu J''} - B_{J'J''} \delta N_{\nu J'}) \tag{14}$$

Integrating over the whole absorption line and neglecting the small change in $\nu$ throughout the line results in

$$\int k_\nu d\nu = \frac{h\nu_0}{4\pi} (B_{J''J'} N_{J''} - B_{J'J''} N_{J'}) \tag{15}$$

where $\nu_0$ is the wave number at the center of the line. By using Eqs. (10) and (11), Eq. (15) can be rewritten as

$$\int k_\nu d\nu = \frac{g_{J'}}{g_{J''}} \frac{A_{J'J''} N_{J''}}{8\pi c \nu_0^2} \left[1 - \frac{g_{J''} N_{J'}}{g_{J'} N_{J''}}\right] \tag{16}$$

For gases in equilibrium, the Boltzmann distribution holds, and

Low . Upper

$$\frac{N_{\text{Upper}}}{N_{\text{Lower}}} = \frac{N_{J'}}{N_{J''}} = \frac{g_{J'}}{g_{J''}} \exp\left(\frac{E_{J''} - E_{J'}}{\kappa T}\right) \tag{17}$$

where $E_{J''}$ is the potential energy of the lower electronic vibrational-rotational state, $E_{J'}$ is the energy of the upper $J'$ state, $\kappa$ is Boltzmann's constant, and T is the gas temperature. For the ultraviolet spectral region, $E_{J''} - E_{J'} \sim -40{,}000\ \text{cm}^{-1}$, $\kappa = 0.695\ \text{cm}^{-1}/°\text{K}$, and for the temperatures encountered (300 to 3000°K), the exponential is very small. Thus $N_{J'}/N_{J''} < 10^{-7}$, and the term in parenthesis in Eq. (16) is approximately unity. That is,

$$\int k_\nu d\nu = \frac{g_{J'}}{g_{J''}} \frac{N_{J''} A_{J'J''}}{8\pi c \nu_o^2} \tag{18}$$

The spontaneous transition probability ($A_{J'J''}$) is related to a term most used in the literature, the oscillator strength, or f-value, through the equation (Ref. 1):

$$\frac{\pi e^2}{mc^2} N_{J''} f_{J'J''} = \frac{g_{J'}}{g_{J''}} \frac{N_{J''} A_{J'J''}}{8\pi c \nu_o^2} \tag{19}$$

where m is the electron mass and e is the electron charge. Substituting Eq. (19) into Eq. (18) then gives

$$\int k_\nu d\nu = \frac{\pi e^2}{mc^2} N_{J''} \bar{f}_{J'J''} \tag{20}$$

## 2.4 SPECTRAL LINE SHAPE

Equation (20) expresses the integral of the absorption coefficient in terms of the population density of the lower rotational state of the absorbing gas ($N_{J''}$) which is a function of the density of the absorbing species and the temperature, and $f_{J'J''}$, which is a constant of the molecule. However, an explicit expression for $k_\nu$ or $\int k_\nu d\nu$ in terms of the measured transmittance or absorption must be obtained in order to use this relationship. An examination of the processes that contribute to the formation of an absorption line of a gas will yield information leading to such an expression.

There are, in general, five processes which contribute to the definition of the shape of an absorption or emission line. Each process can

be regarded as an agent for perturbing the energy levels associated with the transition. The result is a broadening of the line. The five processes are:

1. Natural broadening, due to the finite lifetime of the excited state.
2. Doppler broadening, due to the motions of the molecules.
3. Lorentz broadening, due to collisions with foreign gases.
4. Holtsmark broadening, due to collisions with other absorbing molecules of the same kind.
5. Stark broadening, due to collisions with electrons and ions.

Processes 1 and 5 may be neglected for the temperature range being considered since they contribute much less to the broadening than processes 2, 3, and 4. Processes 3 and 4 have generally been grouped together under the name "pressure" broadening. Thorson and Badger (Ref. 4) have shown that pressure broadening in the bands of NO is much less than Doppler broadening at temperatures greater than room temperature and at pressures less than atmospheric. Therefore, for the work reported here, pressure broadening was neglected and to a very good approximation, Doppler broadening is the only process which contributes to the formation of absorption lines for the NO $\gamma$-bands. For the OH molecule, this is not the case, and the combined Doppler and pressure broadening had to be considered (Refs. 2 and 3).

When Doppler broadening is the dominant mechanism the absorption coefficient is given by (Ref. 1):

$$k_\nu = k_{\nu_o} \exp\left[-\frac{2(\nu - \nu_o)}{\Delta\nu_D}\sqrt{\ln 2}\right]^2 \tag{21}$$

where $\Delta\nu_D$ is the Doppler half-width at half of $k_{\nu_o}$, the maximum absorption coefficient, and $\Delta\nu_D$ depends only on the absolute temperature (T), the central wave number ($\nu_o$), and the molecular mass (M) of the absorbing species, according to the relation

$$\Delta\nu_D = 2\nu_o \frac{\sqrt{2\kappa T \ln 2}}{mc^2} \tag{22}$$

Integrating Eq. (21) over $\nu$ yields the result

$$\int_0^\infty k_\nu d\nu = \tfrac{1}{2}\sqrt{\pi/\ln 2}\, k_{\nu_o} \Delta\nu_D \tag{23}$$

Equating the right hand sides of Eqs. (20) and (23) gives

$$\tfrac{1}{2}\sqrt{\pi/\ln 2}\, k_{\nu_o} \Delta\nu_D = \frac{\pi e^2}{mc^2} N_{J''} f_{J'J''} \tag{24}$$

Now, rewriting Eq. (24) in terms of the absorption coefficient at the line center ($k_{\nu_o}$), the Doppler width ($\Delta\nu_D$), and known properties of the molecule results in

$$N_{J''} = \frac{1}{2\sqrt{\pi \ln 2}} \frac{mc^2}{e^2} \frac{k_{\nu_o} \Delta\nu_D}{f_{J'J''}} \tag{25}$$

It should be noted at this point that the assumption of a Doppler line shape has imposed a very useful property for the measurement technique. In Eq. (25), $N_{J''}$ has been simply related to the absorption coefficient at line center ($k_{\nu_o}$) so that some contrivance which enables this measurement to be made is a necessary part of the technique. Then, Eq. (7) is applicable, and $k_{\nu_o}$ can easily be determined experimentally. The measurement can be accomplished if the source in Fig. 1 is composed of lines having the same wavelength as those of the species to be measured, which are very narrow compared with the width of the absorption lines. One way in which this may be accomplished is through use of a resonance lamp containing the species of interest in which the temperature of the source is much less than the temperature of the absorbing medium. Even when the source lines are of comparable width to those of the absorber, the integrals in Eq. (8) can be solved if the incident line shape and the absorption line shape are known. A solution of Eq. (8) for the case of Doppler line shapes is given in Appendix I where it is shown that the measured transmission can be expressed in terms of the line center transmission ($t_{\nu_o}$).

A second feature of being able to express the integral of the absorption coefficient in terms of the absorption coefficient at line center is that the applicable measurement expression for variation of $k_{\nu_o}$ over the path is

$$t_m = \exp\left(-\int k_{\nu_o} d\ell\right) \tag{26}$$

where $k_{\nu_o}$ is a function of the density and temperature along the path as expressed in Eq. (25). This expression is now amenable to the geometric treatment of Abel inversion for axisymetric flow streams (Ref. 3). That is,

$$\ln \frac{1}{t_m} = \int_L k_{\nu_o} d\ell \tag{27}$$

which, for an axisymetric source, can be inverted to (Ref. 3):

$$k_{\nu_o}(r) = -\frac{1}{\pi}\int_r^R \frac{\frac{d}{dy}(\ln t_m^{-1})dy}{\sqrt{r^2 - y^2}} \tag{28}$$

where r is the radius, y is the distance from the axis where the measurement is made, and R is the full radius of the axisymetric source.

## 2.5 EQUATION FOR THE SPECIES CONCENTRATION

Under conditions of rotational equilibrium, Tatum (Ref. 5) gives expressions for the number density of diatomic molecules in a rotational-vibrational-electronic state satisfying Hund's case "b" as

$$\frac{N_{J''}}{N_o} = \left[\frac{2(2S+1)\exp(\mathcal{T}_e/\kappa T)}{\sum\limits_{\substack{\text{all } n\\ \text{states}}} 2(2S+1)\exp(-\mathcal{T}_{e_n}/\kappa T)}\right]\left[\frac{\exp[-G(v'')/\kappa T]}{\sum\limits_{\substack{\text{all } v\\ \text{states}}} \exp[-G(v'')/\kappa T]}\right]\left[\frac{(2J''+1)\exp[-F(J'')/\kappa T]}{(2S+1)\sum\limits_{J''=0}^{\infty}(2J''+1)\exp[-F(J'')/\kappa T]}\right] \tag{29}$$

where the new terms used are defined as follows:

S is the electron spin angular momentum quantum number

$\mathcal{T}_e$ is the term energy of the electronic state

$G(v'')$ is the vibrational energy of the $\nu''$th vibrational state

$F(J'')$ is the rotational energy of the $J''$th rotational state

$N_o$ is the total number density of the absorbing species.

The first term in brackets goes to unity for a gas in which only the ground electronic state is populated as is the case in this study. The summations are usually identified as the partition functions for electronic,

$$Q_e = \sum_{o}^{\infty} 2(2S + 1) \exp[-\mathcal{T}_n/\kappa T] \quad . \tag{30}$$

vibration,

$$Q_v = \sum_{v=0}^{\infty} \exp[-G(v'')/\kappa T] \tag{31}$$

and rotation,

$$Q_R = \sum_{J''=0}^{\infty} (2J'' + 1) \exp[-F(J'')/\kappa T] \tag{32}$$

Substitution of Eq. (29) into Eq. (25) gives

$$\frac{N_o \exp[-G(v'')/\kappa T]}{Q_v Q_R} \frac{2J'' + 1}{2S + 1} \exp[-F(J'')/\kappa T] = \frac{1}{2\sqrt{\pi \ln 2}} \frac{mc^2}{e^2} \frac{k_{\nu_o} \Delta\nu_D}{f_{J'J''}} \tag{33}$$

Rearrangement of terms in Eq. (33) then yields an equation for the total number density of the species:

$$N_o = \frac{mc^2/e^2}{\sqrt{4\pi \ln 2}} \frac{Q_v}{\exp[-G(v'')/\kappa T]} \frac{2S + 1}{2J'' + 1} \frac{Q_R}{f_{J'J''} \exp[-F(J'')/\kappa T]} k_{\nu_o} \Delta\nu_D \tag{34}$$

Hence, if a single rotational line of known oscillator strength can be isolated and $k_{\nu_o}$ and T can be measured, the number density ($N_o$) of the absorbing species may be determined.

## 2.6 EXPRESSION FOR THE OSCILLATOR STRENGTH

The oscillator strength of a rotational line ($f_{J'J''}$) is defined throughout the literature in varying forms. The nomenclature, and hence consistent formulas for the calculation of rotational oscillator strengths, is a much confused subject. The definition of the oscillator strength as used by Schadee (Ref. 6) with the normalization used by Tatum (Ref. 5) will be used in this work. The vibrational oscillator strength ($f_{v'v''}$) is defined by

$$f_{v'v''} = f_{e\ell} q_{v'v''} \tag{35}$$

where $q_{v'v''}$ is the square of the vibrational overlap integral and is known as the Franck-Condon factor. For molecules for which vibrational constants have been accurately measured for several vibrational states, $q_{v'v''}$ can be accurately calculated. Most measurements of the oscillator strength give a value of a particular $f_{v'v''}$ so that $f_e$ can then be found.

The rotational oscillator strength is given by

$$f_{J'J''} = f_{v'v''} \frac{\lambda_{v'v''}}{\lambda_{J'J''}} \frac{\delta_{J'J''}}{(2J''+1)(2)(2S+1)} \tag{36}$$

where $\lambda_{v'v''}/\lambda_{J'J''}$ is the ratio of the wavelength at the band head to the wavelength of the particular rotational line of interest. $\delta_{J'J''}/(2J''+1)$ is the normalized Hönl-London Factor for which Earls (Ref. 7) and Kovacs (Ref. 8) give formulas for most transitions encountered. Now, substituting Eq. (36) into Eq. (34) gives

$$N_o = \frac{mc^2/e^2}{\sqrt{4\pi \ln 2}} \frac{2(2S+1)^2 Q_v Q_r}{\exp[-G(v'')/\kappa T]} \frac{\lambda_{J'J''}}{\lambda_{v'v''}} \frac{k_{\nu_o} \Delta\nu_D}{\delta_{J'J''} \exp[-F(J'')/\kappa T]} \tag{37}$$

which is the general working equation for narrow line absorption.

## SECTION III
## APPLICATION TO THE NO MOLECULE

A considerable amount of literature exists on the energy level structure of the NO molecule. This section is devoted to the definition of the energy levels and transition probabilities of the NO molecule applicable to this study.

### 3.1 ENERGY LEVELS

The ground electronic energy level of the NO molecule is a doublet $\Pi$ state, denoted by $X'\,^2\Pi$. All the upper electronic energy levels which have been observed are also doublet states and are denoted by $A\,^2\Sigma^+$, $B\,^2\Pi$, $C\,^2\Sigma^+$, $D\,^2\Sigma^+$, and $E\,^2\Sigma^+$ in order of increasing energy. The electronic transitions that have been observed are listed as follows (Ref. 9):

| Transition | Designation |
|---|---|
| $A\ ^2\Sigma^+ \rightarrow X\ ^2\Pi$ | $\gamma$ system |
| $B\ ^2\Sigma^+ \rightarrow X\ ^2\Pi$ | $\beta$ system |
| $C\ ^2\Sigma^- \rightarrow X\ ^2\Pi$ | $\delta$ system |
| $D\ ^2\Sigma^+ \rightarrow X\ ^2\Pi$ | $\epsilon$ system |

The energy level diagram showing the electronic energy levels and the transitions to the ground state, producing the $\gamma$, $\beta$, $\delta$, and $\epsilon$ band systems, is shown in Fig. 3.

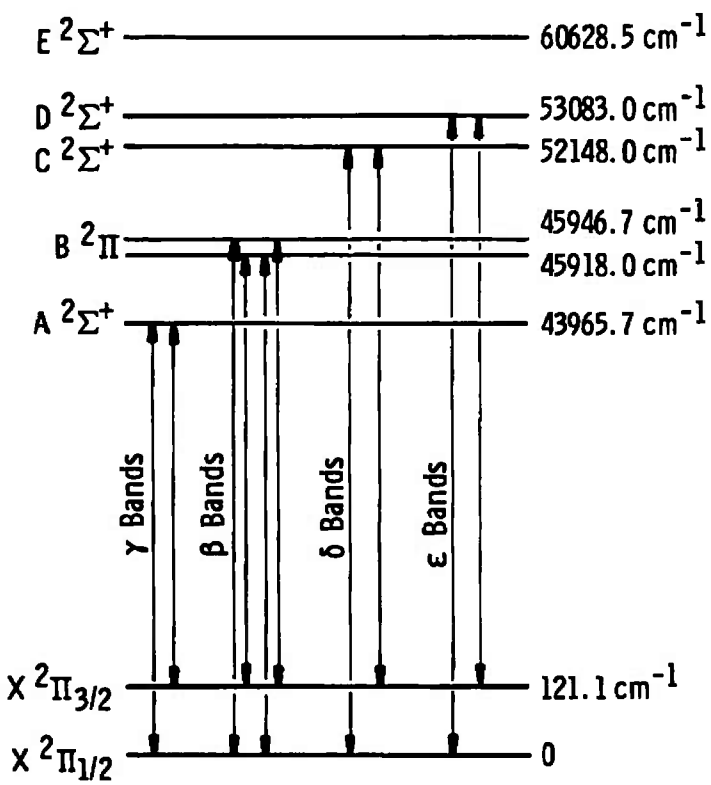


**Fig. 3 Electronic Energy Level Diagram of NO Molecule Indicating the Various Band Systems**

The applicable equations for determining the various vibrational and rotational energy levels and the vibrational and rotational constants for the NO molecule are given generally by Herzberg (Ref. 10). The majority of work with the NO molecule has dealt with the $\gamma$ and $\beta$ systems. Gero and Schmid (Ref. 9) have listed frequencies for

rotational lines in several bands of the $\gamma$ and $\beta$ systems and Deezsi (Ref. 11) has published a more comprehensive analysis of the Gero and Schmid data. Additionally, Gero, Schmid, and Von Szily (Ref. 12) give excellent data for the $\epsilon$ system and also locate rotational lines for a number of bands in this system. For the present work, the $\gamma$ band system of NO was chosen because the wavelength region (2200 to 2400 Å) is more easily accessible than for the other, shorter wavelength bands and because the molecular constants are known more accurately.

In general, the equation for the energy levels of a given electronic energy term has the form

$$\mathcal{T} = \mathcal{T}_e + G(v) + F_n(J) \tag{38}$$

for which $\mathcal{T}_e$ is the ground state electronic energy for that level, G(v) includes the vibrational terms, and $F_n(J)$, the rotational terms.

G(v) has the form,

$$G(v) = \omega_e(v + \tfrac{1}{2}) - \omega_e x_e(v + \tfrac{1}{2})^2 + \omega_e y_e(v + \tfrac{1}{2})^3 + \cdots \tag{39}$$

where $\omega_e$, $\omega_e x_e$, and $\omega_e y_e$ are vibrational constants (Ref. 10). Values of $\mathcal{T}_e$ and the vibrational constants for the A $^2\Sigma^+$ and X $^2\Pi$ states are given in Table I. Note in Table I that $\omega_e$, as given by Gillette and Eyster (Ref. 13), is slightly different for the X $^2\Pi_{1/2}$ and X $^2\Pi_{3/2}$ states.

For doublet states, the term $F_n$ refers to the two electron spin components, $F_1(K - 1/2)$ and $F_2(K + 1/2)$. The ground electronic energy level (X $^2\Pi$) is intermediate between Hund's cases (a) and (b) (Ref. 13). The Hill and Van Fleck equation for the rotational energy levels for the intermediate case as expressed by Churchhill, Hagstrom, and Landshoff (Ref. 14) is applicable to the X $^2\Pi$ state:

$$F_n(J'') = B_v[(J'' + \tfrac{1}{2})^2 - 1 + (-1)^n u] - \begin{cases} D_v J''^4 & n = 1 \\ D_v(J'' + 1)^4 & n = 2 \end{cases} \tag{40}$$

where

$$B_v = B_e - \alpha_e(v + \tfrac{1}{2}) \tag{41}$$

$$D_v = D_e + \beta_e(v + \tfrac{1}{2}) \tag{42}$$

$$U = [(J'' + \tfrac{1}{2})^2 - Y_v(1 - Y_v/4)]^{1/2} \tag{43}$$

$$Y_v = A/B_v \tag{44}$$

The constants ($B_e$, $\alpha_e$, $D_e$, $\beta_e$, and A) for these equations as given in Ref. 13 are included in Table I.

**TABLE I**
**MOLECULAR CONSTANTS USED TO CALCULATE SPECTRAL LINE WAVELENGTHS AND INTENSITIES FOR THE NO $\gamma$-BANDS**

| Molecular Constants, $cm^{-1}$ | $X\ ^2\Pi_{1/2}$ | $X\ ^2\Pi_{3/2}$ | $A\ ^2\Sigma$ |
|---|---|---|---|
| $\mathcal{T}_e$ | 62.1 | 62.1 | 43965.7 |
| $\omega_e$ | 1904.03 | 1903.68 | 2374.8 |
| $\omega_e x_e$ | 13.97 | 13.97 | 16.46 |
| $\omega_e y_e$ | negligible | negligible | negligible |
| $B_e$ | 1.7046 | 1.7046 | 1.9972 |
| $\alpha_e$ | 0.0178 | 0.0178 | 0.01928 |
| $D_e$ | $5 \times 10^{-6}$ | $5 \times 10^{-6}$ | negligible |
| $\beta_e$ | negligible | negligible | negligible |
| $\Gamma$ | --- | --- | negligible |
| A | 124.2 | 124.2 | --- |
| Ref. | 13 | 13 | 15 |

The upper electronic energy level ($A\ ^2\Sigma^+$) of the $\gamma$-system belongs to Hund's case (b) as do all $\Sigma$ states (Ref. 10). The equations for the rotational energy levels of $A\ ^2\Sigma^+$ states are given by Ref. 10 as

$$F_1(J') = B_v(J'-\tfrac{1}{2})(J'+\tfrac{1}{2}) + \tfrac{1}{2}\Gamma(J'-\tfrac{1}{2}) - D_v(J'-\tfrac{1}{2})^2(J'-\tfrac{1}{2})^2 \tag{45}$$

$$F_2(J') = B_v(J'+\tfrac{1}{2})(J'+\tfrac{3}{2}) - \tfrac{1}{2}\Gamma(J'+\tfrac{3}{2}) - D_v(J'+\tfrac{1}{2})^2(J'-\tfrac{3}{2})^2 \tag{46}$$

where $F_1(J')$ refers to the components with $J' = K' + 1/2$, and $F_2(J')$ refers to the components with $J' = K' - 1/2$. The splitting constant is $\Gamma$ and, for NO, may be assumed negligible compared with $B_v$. The other constants for the $A\ ^2\Sigma^+$ level as derived from rotational analysis by Barrow and Miescher (Ref. 15) are given in Table I.

### 3.2 SPECTRAL LINES IN THE $\gamma$-SYSTEM

The energy of a transition between two levels of a band system is expressed by

$$\nu = \mathcal{T}(v', J') - \mathcal{T}(v'', J'') \tag{47}$$

The selection rules ($\Delta\nu' = \nu' - \nu'' = 0, 1, 2, \ldots$ and $\Delta J = J' - J'' = 0, \pm 1$) apply to Eq. (47). By convention, branches of the band for which $\Delta J = 0$ are designated Q branches; for $\Delta J = +1$ they are R branches, and for $\Delta J = -1$ they are P branches. As noted earlier, both electronic energy levels of the system are split into an $F_1$ and an $F_2$ level. Because of this, there are then 12 possible transitions which will obey the selection rule. The 12 possible transitions to some $J''$ level in the $v = 0$ vibrational level of the $X\,^2\Pi_{1/2,3/2}$ state are illustrated in Fig. 4. The designation of the various possible transitions shown in Fig. 4 consists of labeling the line as the P, Q, or R branch with subscripts which designate the $F_1'$ or $F_2'$ transition to the appropriate $F_1''$ or $F_2''$ rotational state. That is, $P_{11}(J'')$ refers to a transition from $F_1'(J'' - 1)$ to $F_1''(J'')$, $R_{21}(J'')$ refers to a transition from $F_2'(J'' + 1)$ to $F''(J'')$, etc.

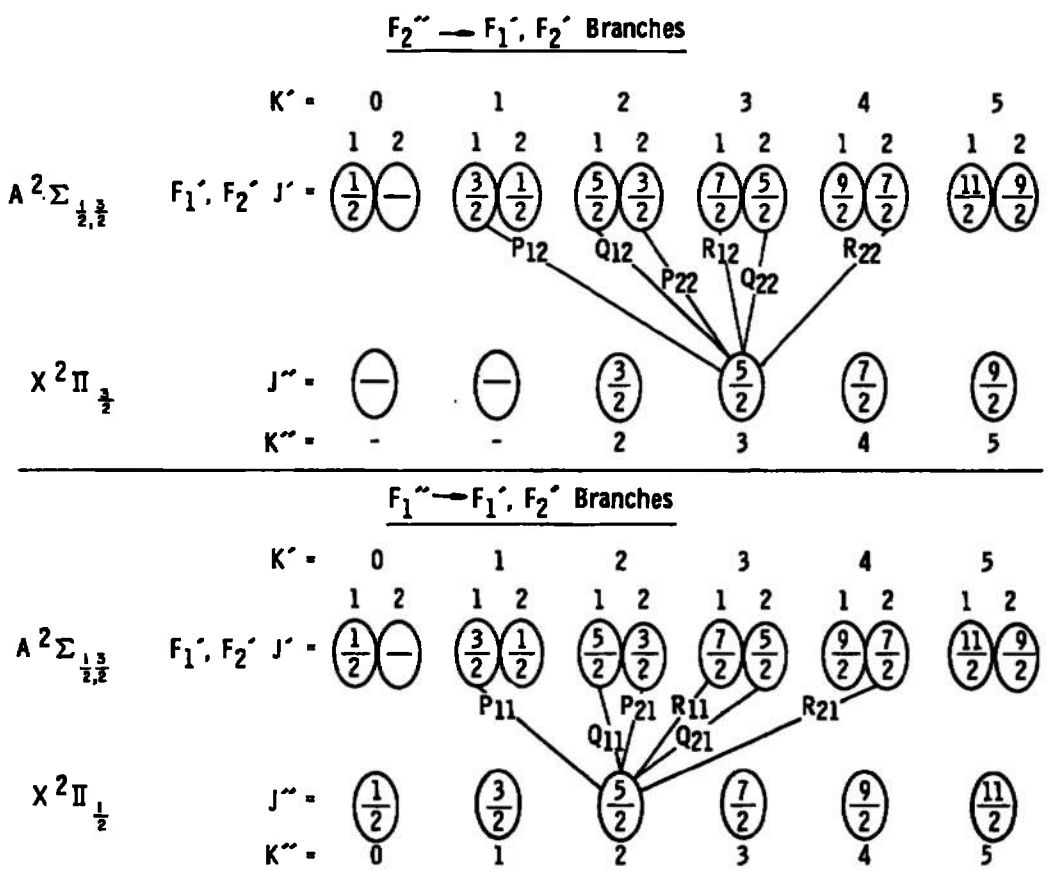


**Fig. 4 Allowed Transitions for NO γ-Bands**

The spectral lines for the $v' = 0$ vibrational level of the $A\ ^2\Sigma^+$ state to the $v'' = 0$ level of the $X\ ^2\Pi$ state were calculated using Eq. (47) and the term formulas for each state given in Eqs. (40), (45), and (46) by means of a computer program written for the IBM 370-155 digital computer. The computer program is described in Appendix II. The calculated lines are shown in Fig. 5 in a way such that the individual lines can be identified. It will be observed that three distinct bandheads appear at 2269.7, 2268.6, and 2263.7 Å. Also, it can be seen that there is much overlapping of lines so that resolution of only a few individual lines is possible.

The computer program described in Appendix II also has the capability to simulate emission spectra that would be obtained from a real spectrometer. The program requires as inputs the oscillator strengths, or transition probabilities of the individual rotational lines of the bands

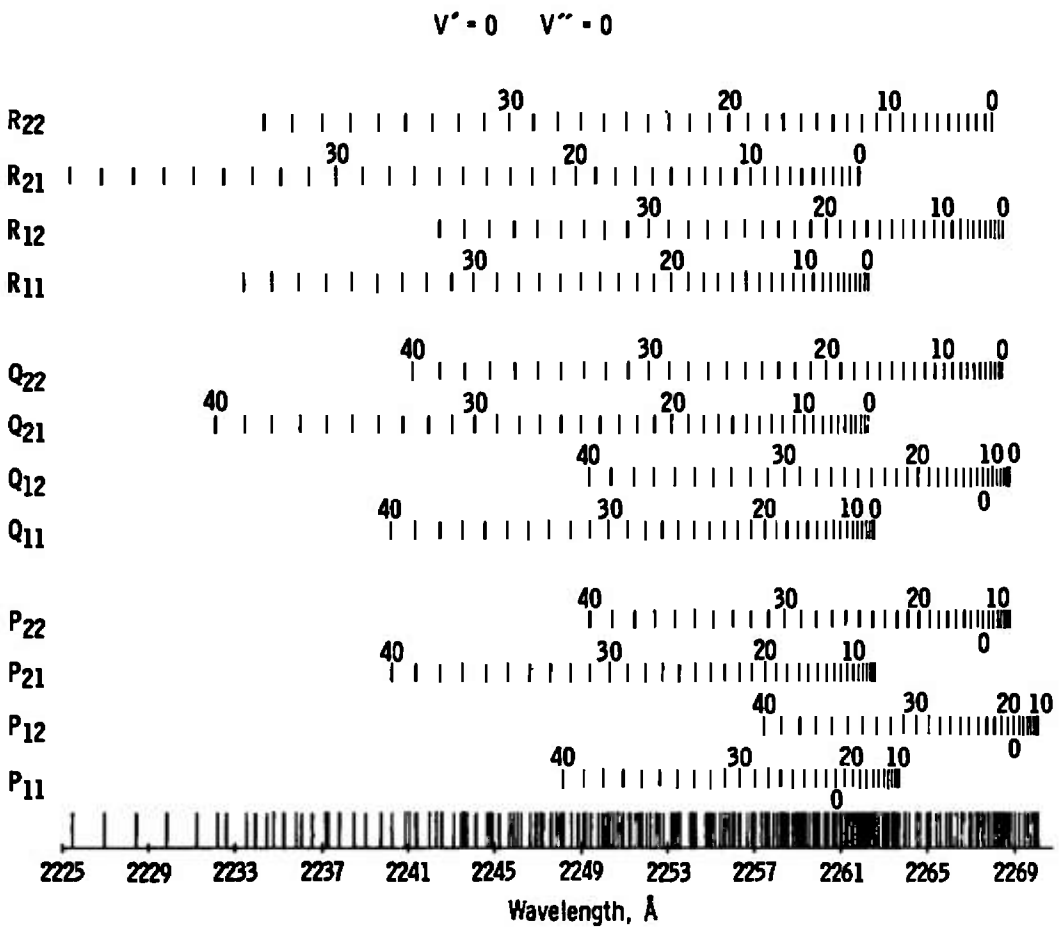


**Fig. 5 Computer-Generated Band Structure for the NO (0,0) γ-Band**

of interest, the temperature, and the instrument slit function. For the calculations presented in Appendix II, the oscillator strengths given in the next section for the NO molecule were used. The temperature was chosen as 775°K, which is characteristic of the source of radiation used (see Section IV). The instrument slit function was taken as triangular with a half-width of 0.03 Å, which corresponds to the slit width of the spectrometer used in the work reported here. The simulated spectrum of the (0,0) band of the γ-system appears in Fig. 6 in two plots, one having a slit function of zero half-width and one having the realistic, 0.03 Å half-width. The simulated spectrum is also characterized by the three distinct bandheads. Between these bandheads several distinct peaks are found which contain groupings of rotational lines. Some of these distinguishable peaks contain only two or three lines. Several peaks useful for measurements are designated in Fig. 6 as 1, 2, 3, etc., and the line components of the peaks are listed, together with their relative strength, in Table II. At wavelengths shorter than that of the $P_{11}$ bandhead, the lines are badly overlapped and not useful for individual line measurements.

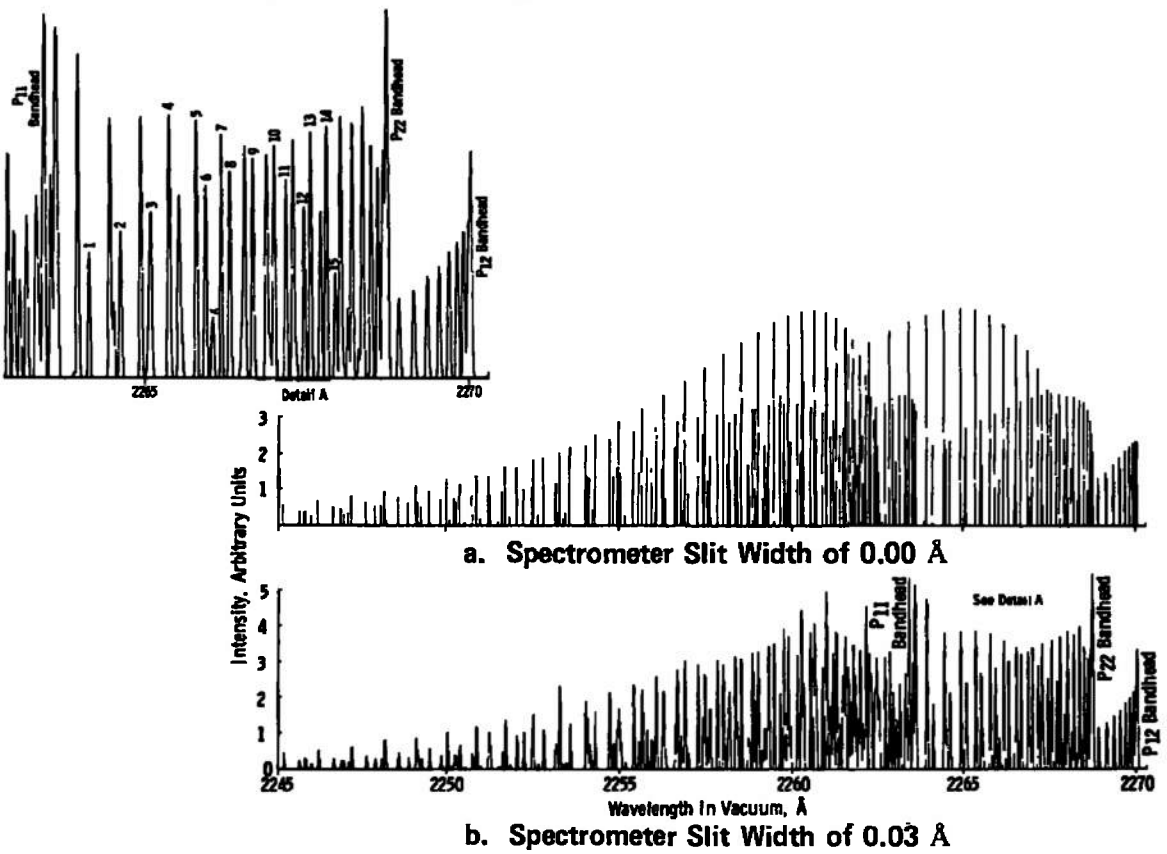


**Fig. 6 Computer-Simulated Spectra for the NO (0,0) γ-Band at a Temperature of 775°K**

## TABLE II
## LINE IDENTIFICATION AND DATA FOR SPECTRAL PEAKS USEFUL FOR NO CONCENTRATION MEASUREMENTS

| Components | Wavelength (Å) | $E(J'')$ ($cm^{-1}$) | $\Sigma S_{J''}$ | $[\lambda \Sigma S_{J''} \exp(-E_{J''}/203.7)]^{-1}$ x $10^{14}$ | C x $10^{15} cm^{-3}$ |
|---|---|---|---|---|---|
| 1-$P_{22}+Q_{12}(43/2)$ | 2264.14 | 829.60 | 17.12+10.38=27.50 | 9.419 | 14.618 |
| 2-$P_{22}+Q_{12}(41/2)$ | 2264.64 | 755.80 | 16.18+10.26=26.44 | 6.786 | 10.532 |
| 3-$P_{22}+Q_{12}(39/2)$ | 2265.11 | 685.43 | 15.25+10.12=25.37 | 5.016 | 7.784 |
| 4-$Q_{22}+R_{12}(23/2)$ | 2265.40 | 288.75 | 14.95+3.38=18.33 | 0.991 | 1.538 |
| 5-$Q_{22}+R_{12}(21/2)$ | 2265.82 | 245.80 | 13.38+3.15=16.53 | 0.890 | 1.381 |
| 6-$P_{22}+Q_{12}(35/2)$ | 2265.96 | 554.96 | 13.43+9.76=23.19 | 2.872 | 4.457 |
| x-$R_{22}(11/2)$ | 2266.07 | 82.53 | 2.44=2.44 | 2.712 | 4.209 |
| 7-$Q_{22}+R_{12}(19/2)$ | 2266.21 | 206.28 | 11.85+2.90=14.75 | 0.824 | 1.279 |
| 8-$P_{22}+Q_{12}(33/2)$ | 2266.35 | 494.87 | 12.54+9.54=22.08 | 2.245 | 3.484 |
| 9-$P_{22}+Q_{12}(31/2)$ | 2266.70 | 438.20 | 11.66+9.29=20.95 | 1.791 | 2.780 |
| 10-$P_{22}+Q_{12}(29/2)$ | 2267.03 | 384.95 | 10.81+9.00=19.81 | 1.453 | 2.255 |
| 11-$Q_{22}+R_{12}(13/2)$ | 2267.22 | 108.31 | 7.53+2.03=9.56 | 0.786 | 1.220 |
| 12-$Q_{22}+R_{12}(13/2)$ | 2267.50 | 82.53 | 6.18+1.70=7.88 | 0.839 | 1.302 |
| 13-$P_{22}+Q_{12}(25/2)$ | 2267.60 | 288.75 | 9.14+8.32=17.46 | 1.023 | 1.588 |
| 14-$R_{22}+Q_{12}(23/2)$ | 2267.85 | 245.80 | 8.34+7.92=16.26 | 0.864 | 1.341 |
| 15-$Q_{22}+R_{12}(7/2)$ | 2267.98 | 41.27 | 3.60+0.96=4.56 | 1.184 | 1.838 |

### 3.3 LINES CHOSEN FOR ABSORPTION MEASUREMENTS

The peaks given in Table II and shown in Fig. 6 which contain strong lines terminating in the same lower rotational state were considered to be the most useful for the absorption measurements. These are the groups containing only $Q_{22}(J'') + R_{12}(J'')$ or $P_{22}(J'') + Q_2(J'')$ lines; in other words, those containing only lines originating from a common lower rotational state. For example, the peak designated as 2 contains $P_{22}(41/2) + Q_{12}(41/2)$ lines and the peak designated as 4 contains only $Q_{22}(25/2) + R_{12}(25/2)$ lines. Only one peak was found which contains a single line, $R_{22}(15/2)$, which is marked X in Fig. 6. Other peaks are overlapped mainly with $R_{22}$ branch lines and the computation of $N_o$ would be difficult using these.

### 3.4 OSCILLATOR STRENGTHS FOR THE $\gamma$-SYSTEM

The oscillator strength ($f_{J'J''}$) as defined in Eq. (36) requires knowledge of $f_{v'v''}$ and $\delta_{J'J''}$. Perry-Thorne and Banfield (Ref. 16) have presented the latest results on determination of $f_{00}$, the

vibrational oscillator strength for the (0,0) band of the system. They give $f_{00} = 3.64 \pm 0.05 \times 10^{-4}$. Spindler, Isaacson, and Wentink (Ref. 17) have calculated values of $q_{v'v''}$, which are given in Table III, so that any $f_{v'v''}$ can be determined by use of Eq. (35).

**TABLE III**
**FRANCK-CONDON FACTORS FOR THE γ-BANDS OF NO***

| v′ | v″ | | | | | |
|---|---|---|---|---|---|---|
| | 0 | 1 | 2 | 3 | 4 | 5 |
| 0 | 0.1615** | 0.2586 | 0.2397 | 0.1625 | 0.0912 | 0.0470 |
| | 0.1524*** | 0.2476 | 0.2367 | 0.1688 | 0.0987 | 0.0514 |
| 1 | 0.3336 | 0.1046 | 0.0004 | 0.0675 | 0.1288 | 0.1329 |
| | 0.3277 | 0.1134 | 0.0000+ | 0.0566 | 0.1224 | 0.1319 |
| 2 | 0.2991 | 0.0162 | 0.1517 | 0.0738 | 0.0008 | 0.0310 |
| | 0.3029 | 0.0108 | 0.1444 | 0.0825 | 0.0028 | 0.0236 |
| 3 | 0.1490 | 0.1999 | 0.0443 | 0.0392 | 0.1105 | 0.0514 |
| | 0.1552 | 0.1900 | 0.0543 | 0.0287 | 0.1075 | 0.0583 |
| 4 | 0.0462 | 0.2443 | 0.0438 | 0.1228 | 0.0021 | 0.0541 |
| | 0.0496 | 0.2486 | 0.0329 | 0.1262 | 0.0054 | 0.0442 |
| 5 | 0.0094 | 0.1324 | 0.2217 | 0.0005 | 0.1026 | 0.0468 |
| | 0.0105 | 0.1405 | 0.2134 | 0.0031 | 0.0948 | 0.0545 |

* Taken from Spindler, Isaacson, and Wentink, Ref. 17

** $A\ ^2\Sigma - X\ ^2\Pi_{1/2}$

*** $A\ ^2\Sigma - X\ ^2\Pi_{3/2}$

Earls (Ref. 7) has published formulas for the normalized Hönl-London factors for $^2\Sigma - {}^2\Pi$ transitions, which apply to the γ-system of NO. The expressions are given in Table IV. As noted earlier, the measurement of absorption has to be on pairs of lines originating from the same J″, rather than individual lines. The pairs useful for absorption measurements consist of the $P_{22}$ and $Q_{12}$ lines, and the $Q_{22}$ and $R_{12}$ lines identified in Table II. Churchill, Hagstrom, and Landshoff

## TABLE IV
## HÖNL-LONDON FACTORS FOR $^2\Sigma \rightarrow {}^2\pi$ TRANSITIONS INTERMEDIATE BETWEEN HUND'S CASES (a) AND (b)*

$$R_{22} = \frac{(2J''+1)^2 + (2J''+1)[Y(Y-4) + (2J''+1)^2]^{-1/2}(4J''^2 + 4J'' + 1 - 2Y)}{8(J''+1)}$$

$$Q_{22} = \frac{(2J''+1)[(4J''^2 + 4J'' - 1) + \{Y(Y-4) + (2J''+1)^2\}^{-1/2}(8J''^3 + 12J''^2 - 2J'' + 1 - 2Y)]}{8J''(J''+1)}$$

$$P_{22} = \frac{(2J''+1)^2 + (2J''+1)[Y(Y-4) + (2J''+1)^2]^{-1/2}(4J''^2 + 4J'' - 7 + 2Y)}{8J''}$$

$$R_{12} = \frac{(2J''+1)^2 - (2J''+1)[Y(Y-4) + (2J''+1)^2]^{-1/2}(4J''^2 + 4J'' - 7 + 2Y)}{8(J''+1)}$$

$$Q_{12} = \frac{(2J''+1)[(4J''^2 + 4J'' - 1) - \{Y(Y-4) + (2J''+1)^2\}^{-1/2}(8J''^3 + 12J''^2 - 2J'' - 7 + 2Y)]}{8J''(J''+1)}$$

$$P_{12} = \frac{(2J''+1)^2 - (2J''+1)[Y(Y-4) + (2J''+1)^2]^{-1/2}(4J''^2 + 4J'' + 1 - 2Y)}{8J''}$$

$$R_{11} = \frac{(2J''+1)^2 - (2J''+1)[Y(Y-4) + (2J''+1)^2]^{-1/2}(4J''^2 + 4J'' - 7 + 2Y)}{8(J''+1)}$$

$$Q_{11} = \frac{(2J''+1)[(4J''^2 - 4J'' - 1) + \{Y(Y-4) + (2J''+1)^2\}^{-1/2}(8J''^3 + 12J''^2 - 2J'' - 7 + 2Y)]}{8J''(J''+1)}$$

$$P_{11} = \frac{(2J''+1)^2 + (2J''+1)[Y(Y-4) + (2J''+1)^2]^{-1/2}(4J''^2 + 4J'' + 1 - 2Y)}{8J''}$$

$$R_{21} = \frac{(2J''+1)^2 - (2J''+1)[Y(Y-4) + (2J''+1)^2]^{-1/2}(4J''^2 + 4J'' + 1 - 2Y)}{8(J''+1)}$$

$$Q_{21} = \frac{(2J''+1)[(4J''^2 + 4J'' - 1) - \{Y(Y-4) + (2J''+1)^2\}^{-1/2}(8J''^3 + 12J''^2 - 2J'' + 1 - 2Y)]}{8J''(J''+1)}$$

$$P_{21} = \frac{(2J''+1)^2 - (2J''+1)[Y(Y-4) + (2J''+1)^2]^{-1/2}(4J''^2 + 4J'' - 7 + 2Y)}{8J''}$$

where $Y = A'/B_v$

*Reference 7

(Ref. 14) have taken into account this overlapping of lines and have expressed the Hönl-London factors, where applicable, as the sum of the Hönl-London factor for each line as follows:

$$\Sigma\delta[Q_{22}(J'') + R_{12}(J'')] = \frac{2J''+1}{8J''}[(6J''-1) + U(4J''^2+4J''+1-2Y_v)] \tag{48}$$

$$\Sigma\delta[P_{22}(J'') + Q_{12}(J'')] = \frac{2J''+1}{B(J''+1)}[(6J''+7) - U(4J''^2+4J''+1-2Y_v)] \tag{49}$$

where $J''$ refers to the J-value in the $X\,^2\Pi_{1/2,\,3/2}$ state for a given rotational transition. Here, U has the form

$$U = [Y_v^2 - 4Y_v + (2J''+1)^2]^{-1/2} \tag{50}$$

where $Y_v = A/B_v$ is the coupling factor. For the NO $\gamma$-system, A has a value of 124.2 $cm^{-1}$. The values of $\Sigma\delta_{J''}$ for these line pairs for the lines used in this study are also given in Table II.

## 3.5 MODIFICATION OF SPECTRAL LINE ABSORPTION THEORY FOR MULTIPLETS

Application of Eq. (34) for determining species concentrations requires summing over the two lines of the same wavelength. That is,

$$\sum_{J'}\left(\int_0^\infty k_\nu d\nu\right)_{J'J''} = \sqrt{\pi/4\ln 2}\sum_{J'}(\Delta\nu_D)_{J'J''}(k_{\nu_o})_{J'J''} \tag{51}$$

For a single line,

$$\int_0^\infty k_\nu d\nu = \frac{\pi e^2}{mc^2} N_{J''} f_{J'J''} \tag{52}$$

and for the pair of lines ($Q_{22} + R_{12}$),

$$\sum_{J'}\left(\int k_\nu d\nu\right)_{J'J''} = \frac{\pi e^2}{mc^2}\sum_{J'} N_{J''} f_{J'J''} = \frac{\pi e^2}{mc^2} N_{J''}\Sigma\delta[Q_{22}(J'') + R_{12}(J'')] \tag{53}$$

or, for the pair $P_{22} + Q_{12}$,

$$\sum_{J'}\left(\int k_\nu d\nu\right)_{J'J''} = \frac{\pi e^2}{mc^2} N_{J''}\Sigma\delta[P_{22}(J'') + Q_{12}(J'')]$$

Using Eqs. (45), (46), and (37) and grouping together quantities which explicitly depend on the rotational transitions result in an equation for the concentration:

$$N_o = \frac{mc^2/e^2}{\sqrt{4\pi \ln 2}} \frac{2(2S+1)^2 \; Q_v Q_r}{\exp[-G(v'')/\kappa T]} \frac{\lambda_{J'J''}}{\lambda_{v'v''}} \frac{\Delta\nu_D \sum_{J'} (k_{\nu_o})_{J'J''}}{f_{v'v''} (\sum_{J'} S_{J'J''}) \exp[-F(J'')/\kappa T]} \tag{54}$$

where the quantities $\lambda_{J'J''}$ and $(\Delta\nu_D)_{J'J''}$ are not included under the summations because they are the same for each line in the peak. The definition is made:

$$(\bar{k}_o)_{\nu_o} = \sum_{J'} (k_{\nu_o})_{J'J''} \tag{55}$$

where $(\bar{k}_o)_\nu$ is the measured absorption coefficient. The combination Hönl-London Factor $(\sum_{J'} S_{J'J''})$ is just the sum of the Hönl-London factors for the pair of lines $(Q_{22} + R_{12})$ or $(P_{22} + Q_{12})$, Eqs. (48) and (49).

### 3.6 FINAL WORKING EQUATIONS

The final step in developing a satisfactory working equation for predicting NO concentrations is the determination of the values of the parameters involved. The quantities in Eq. (54) are given as follows, using cgs units:

$$mc^2/e^2 = 3.555 \times 10^{12} \text{ gm cm}^2 \text{ sec}^{-2} \text{ esu}^{-2}$$

$$\sqrt{4\pi \ln 2} = 2.953$$

$$2(2S+1)^2 = 8(S = 1/2)$$

$$Q_v/\exp[-G(v'')/\kappa T] \simeq 1.000 \qquad (T = 293°K)$$

$$Q_r = \sum_{J=0}^{\infty} (2J+1) \exp[-F(J)/\kappa T] \simeq \kappa T/B_o = 122.2 \qquad (T = 293°K)(\text{Ref. } 10)$$

$$\lambda_{J'J''}/\lambda_{v'v''} \simeq 1$$

$$\Delta\nu_D = 2.228 \times 10^{-6} \lambda^{-1} \text{ cm}^{-1} \qquad (T = 293° K)$$

$$f_{oo} = 3.64 \times 10^{-4} \quad (\text{Ref. } 16)$$

The absorption coefficient at the peak of the absorption line is determined from the relation

$$\bar{k}_{\nu_o} = \frac{1}{L} \ln \left( \frac{I_m^o}{I_m} \right)_{\nu_o} \tag{56}$$

where L, the path length through the absorbing gas, is 45.72 cm (for the absorption tube used). The numerical equation for this measurement is thus obtained:

$$N_o = C \ln \left( \frac{I_m^o}{I_m} \right)_{\nu_o} \tag{57}$$

where

$$C = \frac{7.22 \times 10^{12}}{L\lambda \exp[-E_{J''}/\kappa T] \begin{Bmatrix} S_{J''}(Q_{22} + R_{12}) \\ S_{J''}(P_{22} + Q_{12}) \end{Bmatrix}} = \frac{1.59 \times 10^{11}}{\lambda \exp[-E_{J''}/\kappa T] \begin{Bmatrix} S_{J''}(Q_{22} + R_{12}) \\ S_{J''}(P_{22} + Q_{12}) \end{Bmatrix}} \tag{58}$$

where $\lambda$ is the wavelength at the measured peak in cm. Values of $S_{J''}(Q_{22})$, $S_{J''}(R_{12})$, $S_{J''}(P_{22})$, and $S_{J''}(Q_{12})$ are given in the tabulations for each line in Appendix II, and their sum is given for each of the peaks used for measurements in Table II. The numerical value of the J'' dependent part of Eq. (58) at a temperature of 293°K is also given in Table II.

## SECTION IV
## DESCRIPTION OF EXPERIMENT

### 4.1 APPARATUS

#### 4.1.1 Ultraviolet Spectrometer

A 1-meter Jarrell-Ash grating spectrometer equipped with curved slits was used. The grating had 1180 lines/mm and was blazed at 7500 Å. A Hamamatsu-type R106 photomultiplier tube with S-19 spectral response was used as the detector. The external optics consisted of two fused silica lenses each with an f-number of 4.4. The lenses were placed, as shown in Fig. 7, such that parallel light from the source would pass through the absorbing gas and focus on the slit of

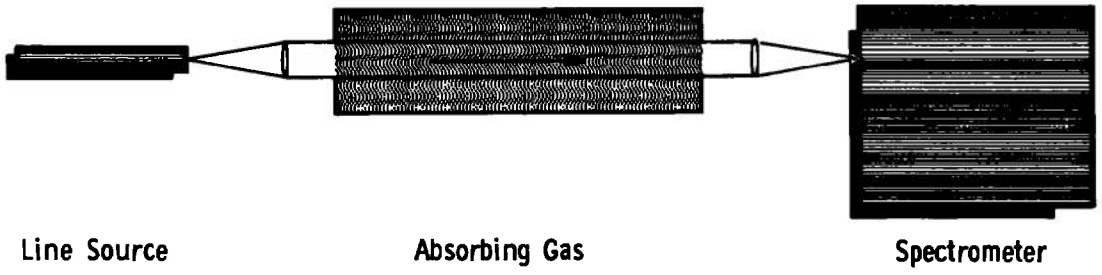


**Fig. 7 Diagram of Experimental Apparatus**

the spectrometer. A physical slit width of $10\mu$ was used for the absorption measurements.

### 4.1.2 Source of NO Radiation

The source used was the discharge from a small, water-cooled capillary tube containing a mixture of A, $N_2$, and $O_2$ at a pressure of approximately 5mm Hg. A Fluke power supply, operated at 2800 v, was used to maintain a discharge which produced the NO radiation. The discharge was viewed along the axis of the tube. A diagram of the discharge tube is presented in Fig. 8.

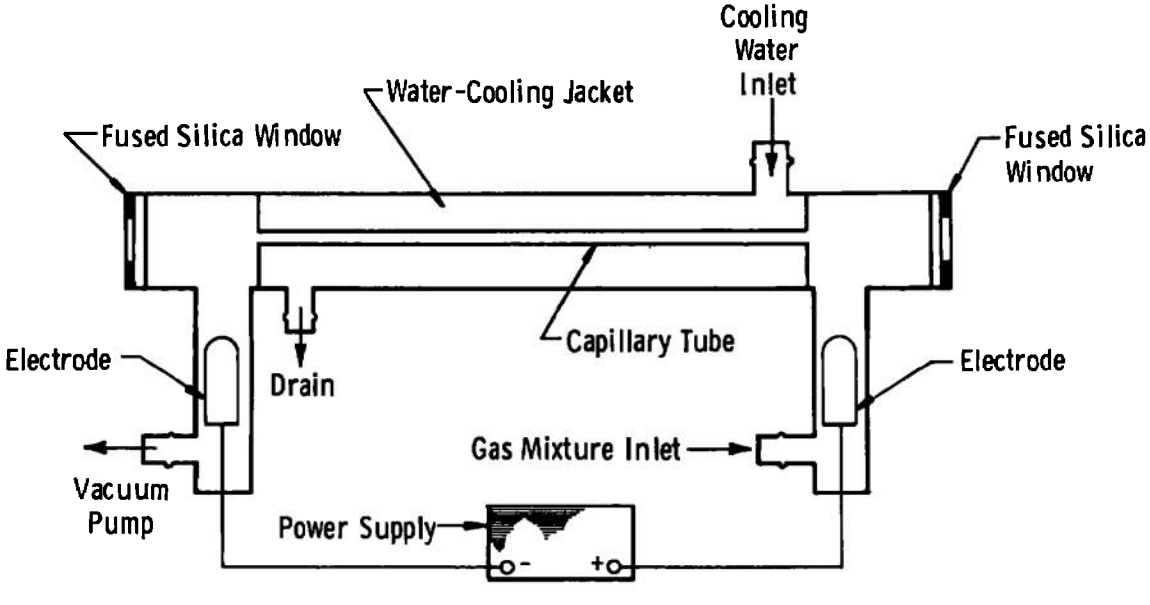


**Fig. 8 Diagram of Discharge Tube Used to Produce NO $\gamma$-Band Radiation**

### 4.1.3 Absorption Cell

The absorption cell was a stainless steel tube approximately 18 in. in length with an inner diameter of 1-7/8 in. Two 1/4-in.-thick fused silica windows were placed at each end. The cell had four stainless steel valves attached as shown in Fig. 9 to provide for evacuating the cell, bleeding in nitric oxide, bleeding in other gases, and isolating the pressure gage. The system was cleaned and dried before use with the NO. The NO was at room temperature which was 294 ± 1°K.

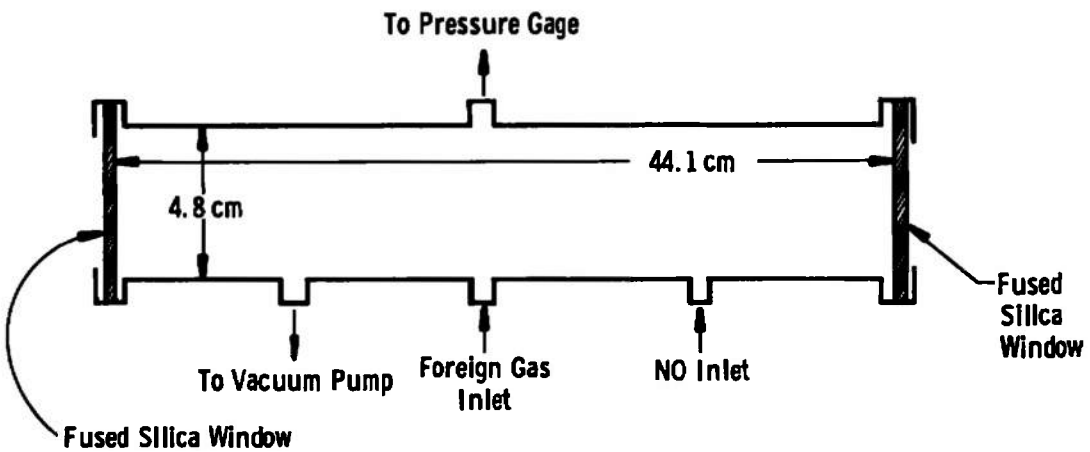


**Fig. 9 Diagram of Absorption Cell Used to Contain Samples of NO at Known Pressure and Temperature**

### 4.1.4 Data Recording System

The data recording system is shown in Fig. 10. A Fluke Model 412-B high-voltage power supply was used to provide excitation voltage for the photomultiplier tube. An operating voltage of 800 v was used because it provided the optimum signal-to-noise ratio. The photomultiplier tube signal was fed into a Philbrick Model P-2 operational amplifier having a gain of 100. The signal was recorded on a Mosely strip-chart recorder which graphically displayed the spectrum. Linearity of the system was checked using a standard potentiometer and found to be within 0.1 percent. The noise level encountered was found to give the largest instrument uncertainty (approximately ±2 percent) in the measurement.

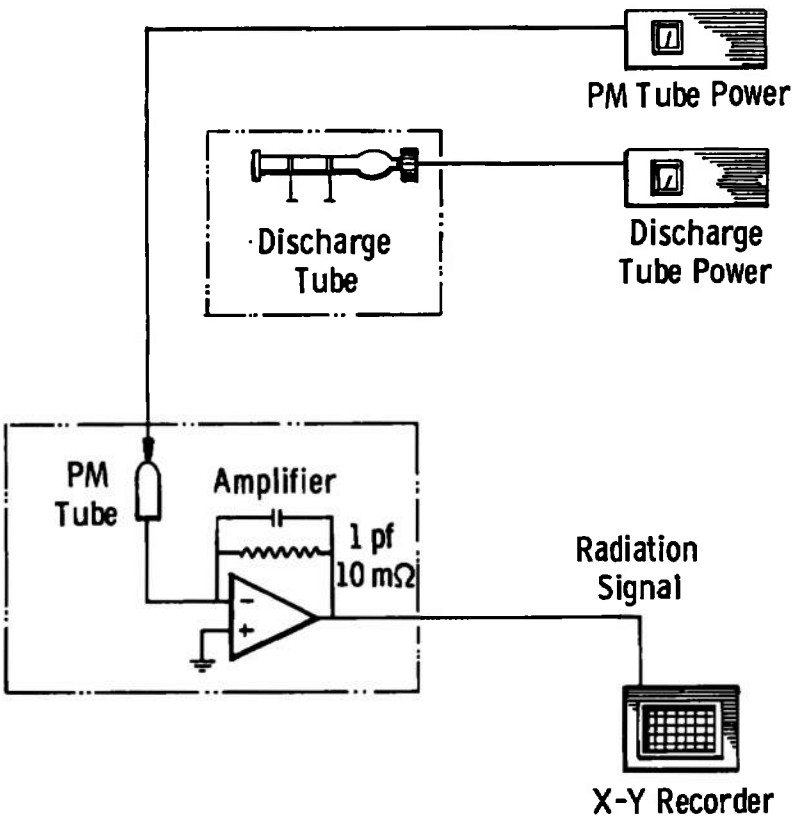


**Fig. 10 Diagram of Data Recording System Used with Spectrometer**

### 4.1.5 Gas Property Instruments

Knowledge of the pressure and temperature of the gas in the absorption cell was important so that number densities of NO molecules could be calculated to use for comparison with values obtained from the absorption measurements. A McLeod vacuum gage was used to measure the pressure. The limiting uncertainty of this gage is the readability, which for the range of pressures employed here, is about ±2.5 percent. The room temperature (assumed equal to the cell temperature) was measured using a mercury thermometer reading in degrees Centigrade. A maximum deviation of one degree from the

observed reading was assumed to be the maximum error. Thus, the maximum uncertainty in the density of the gas in the absorption tube is conservatively estimated to be ±3 percent.

## 4.2 PERFORMANCE OF NO RADIATION SOURCE

The discharge tube was operated using air, mixtures of NO with argon, and mixtures of $N_2$, $O_2$, and argon flowing through the tube at various pressures from about 100 microtorr to 5 torr. The most intense and stable radiation of the $\gamma$-bands was produced when a 12:3:1 mixture of $A:N_2:O_2$ was used at a pressure of 5 torr. The spectrum of the portion of the (0,0) band of interest to this study is shown in Fig. 11. This spectrum was obtained in second order of the 1-meter spectrometer using $10\mu$ slits; under these conditions the resolution was approximately 0.05 Å with a measured equivalent instrument slit width of 0.037 Å. The simulated spectrum calculated for the estimated temperature of the source (373°K) and 0.03 Å instrument slit width is also shown for comparison. Obviously, the calculated line wavelengths and intensities do not exactly correspond to those of the discharge tube, but the comparison is close enough for line identification. The lines previously selected for the absorption measurement are indicated.

## 4.3 PROCEDURE FOR ABSORPTION MEASUREMENTS

The absorption tube was first evacuated to a pressure less than $10^{-3}$ torr and then a base line spectrum covering the wavelength range shown in Fig. 11 was taken. (The base line spectrum was the same with the absorption tube containing air at atmospheric pressure.) Then, the tube was filled with NO at a pressure of about 5 torr, which was found to give absorption of about 90 percent, and the spectral scan, over the wavelength range in Fig. 11, was made. The NO pressure was then reduced by opening the valve to the vacuum pump for a short time, and the spectrum was again obtained. This procedure was repeated over a range of pressures down to 0.018 torr. The pressure in the absorption tube was carefully measured using the McLeod gage for each condition. The tube was then evacuated completely, and a post base line spectra was obtained. In most runs no measurable drift in the intensity of radiation from the discharge tube could be detected.

Attempts were also made to test the effect of increased pressure from non-absorbing gases in the tube. However, it was found that only

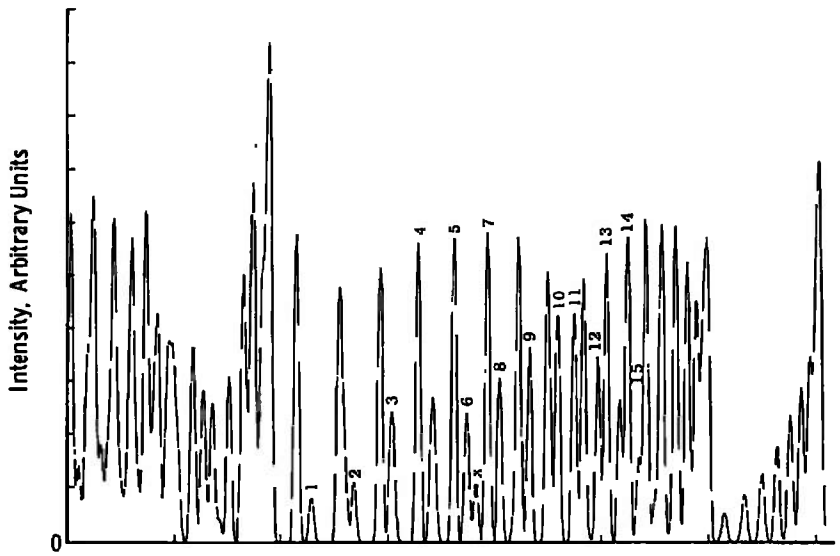


a. Computer-Simulated Spectra, Slit Width of 0.03 Å

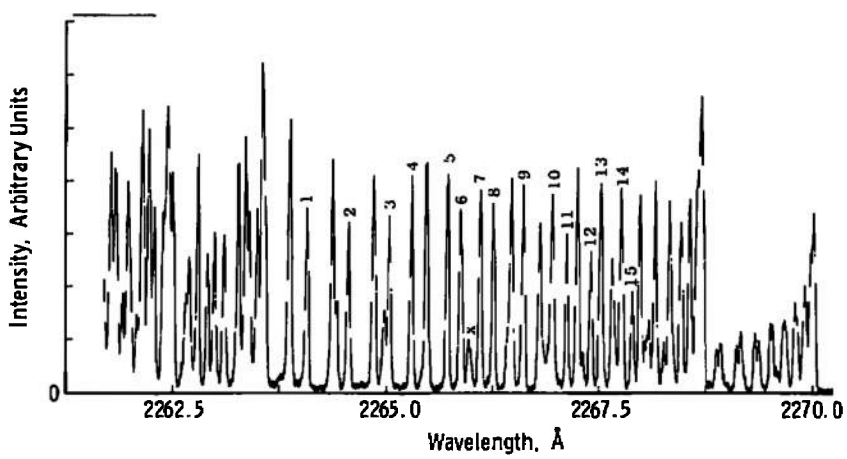


b. Spectrum from Source, Slit Width of 0.03 Å

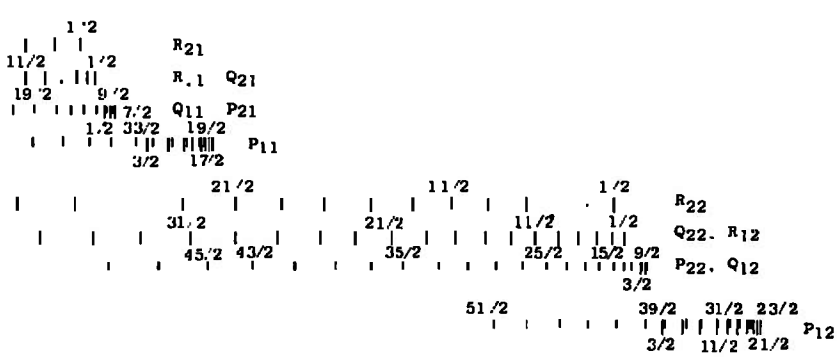


c. Rotational Line Location

Fig. 11 Portion of (0,0) NO γ-Band Used for Narrow Line Absorption Measurements

a few torr of air in the tube was sufficient to destroy the NO in a few seconds. Furthermore, with the system used, enough air was introduced when argon or helium was used as the diluent gas to produce the same effect.

## SECTION V
## RESULTS AND DISCUSSION

### 5.1 Results

A set of spectral scans of the NO (0,0) $\gamma$-band obtained at different pressures in the absorption cell is shown in Fig. 12. The lines used for the absorption measurements and calculations are indicated. The scans are shown in two sets which were run several days apart.

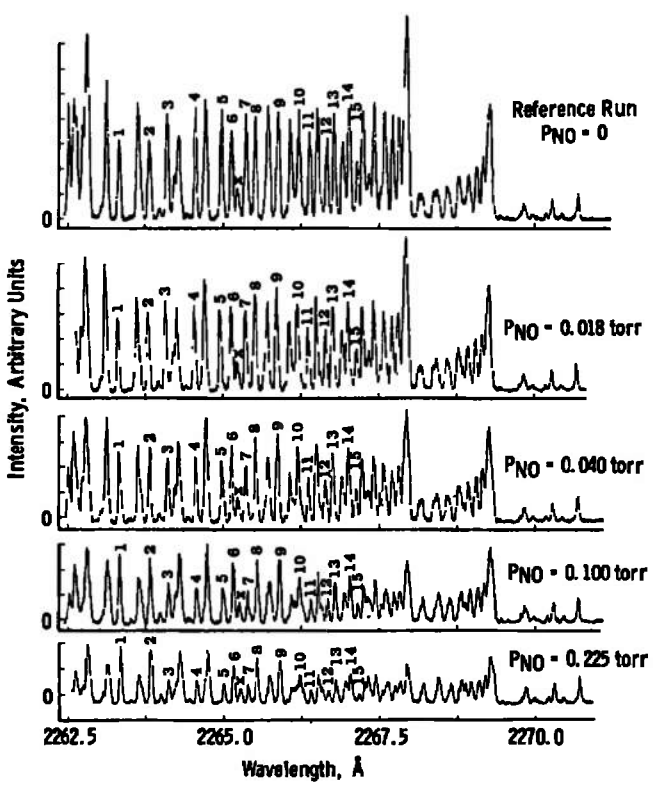


a. Run Number 1

**Fig. 12 Experimental Data from Absorption Measurements of NO $\gamma$-Band Radiation Passing through a Low-Pressure Absorption Tube Containing NO**

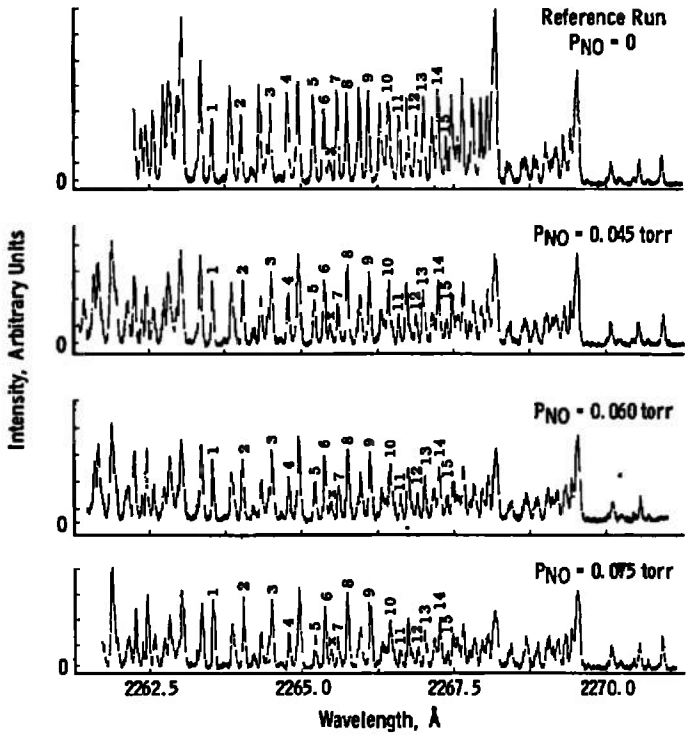


**b. Run Number 2**
**Fig. 12 Concluded**

The calculated density of NO as a function of the transmission $(I_m/I_m^o)_{\nu_o}$ using Eqs. (57) and (58) with the data from Table II is shown in Fig. 13 for several spectral lines. Also shown in Fig. 13 is the transmission at different densities calculated from the data in Fig. 12, and the transmission at line center for each of these data points obtained using the method of Appendix I. Agreement between theory and experiment is considered good (after the conversion from measured transmission to line center transmission is made) for those peaks containing $Q_{22} + R_{12}$ lines from a common $J''$ state when the transmission is greater than about 12 percent. For some reason (possibly overlap from adjacent lines), the $P_{22} + Q_{12}$ lines and the single $R_{22}$ line give poor comparison to the theoretical curve. No consistent trend in the deviation from the theoretical for the $Q_{22} + R_{22}$ lines could be detected, and the deviations from the theoretical curve appear to be no larger than 20 percent.

Equations (57) and (58) may also be written in the form

$$\ln \frac{\ln I_m^o/I_m}{S_{J''}(Q_{22} + R_{12})} = \ln \frac{\lambda}{1.55 \times 10^{-11}} - \frac{E_{J''}}{\kappa T} \tag{59}$$

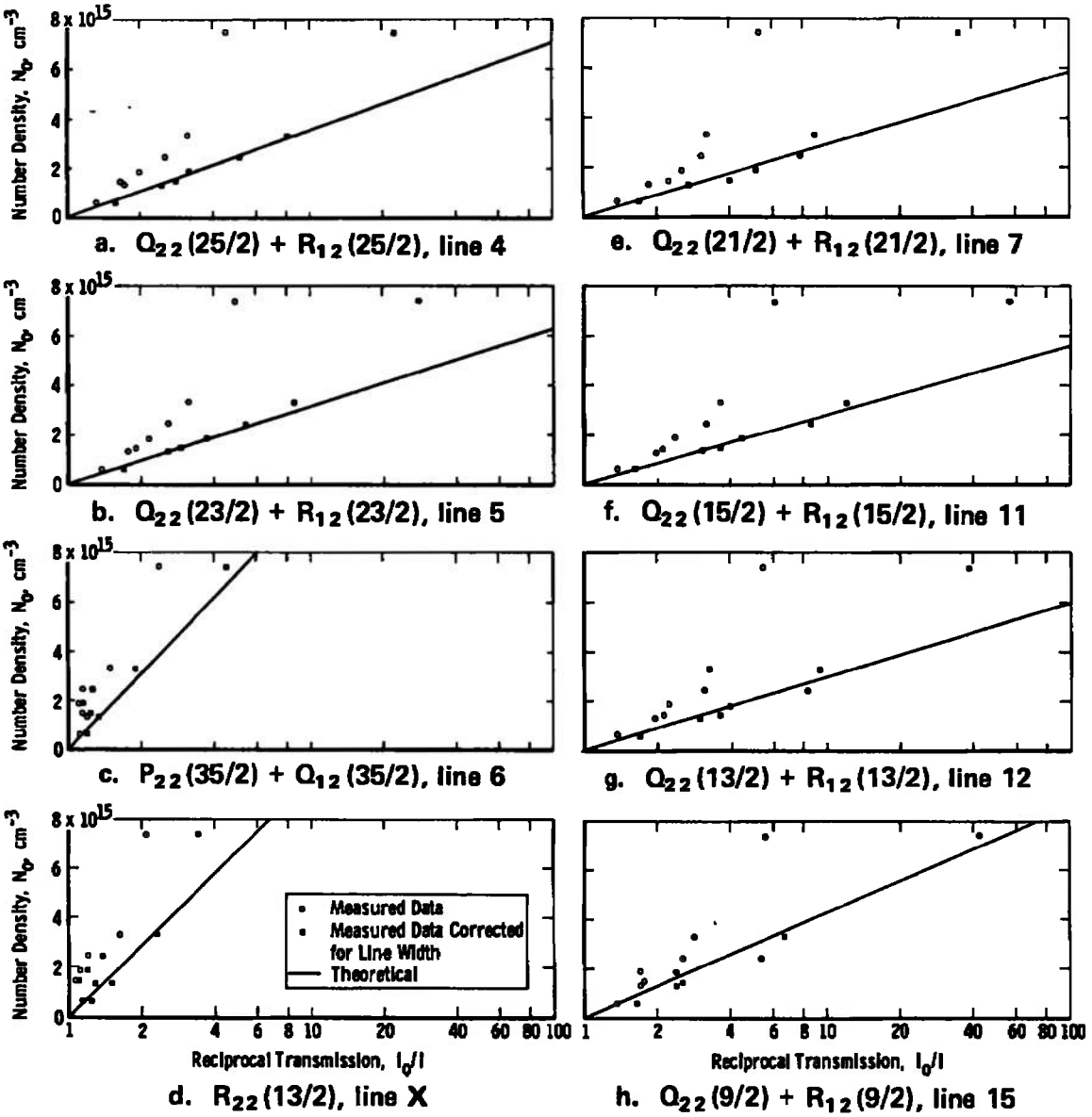


**Fig. 13 Theoretical and Experimental Transmission of Several NO (0,0) γ-Band Lines through NO Gas at Various Pressures**

where only the $Q_{22} + R_{12}$ lines have been included. When the left-hand side of the equation is plotted versus $E_{J''}$, a straight line should result having a slope of $1/\kappa T$, and thus the rotational temperature can be determined. Such a plot for the data of Fig. 13 and using the properties of Table II is given in Fig. 14. The least-squares straight line shown gives a temperature of 293°K, that is, room temperature. This result serves as a check on the method and also shows that the absorption data can be used for temperature measurement.

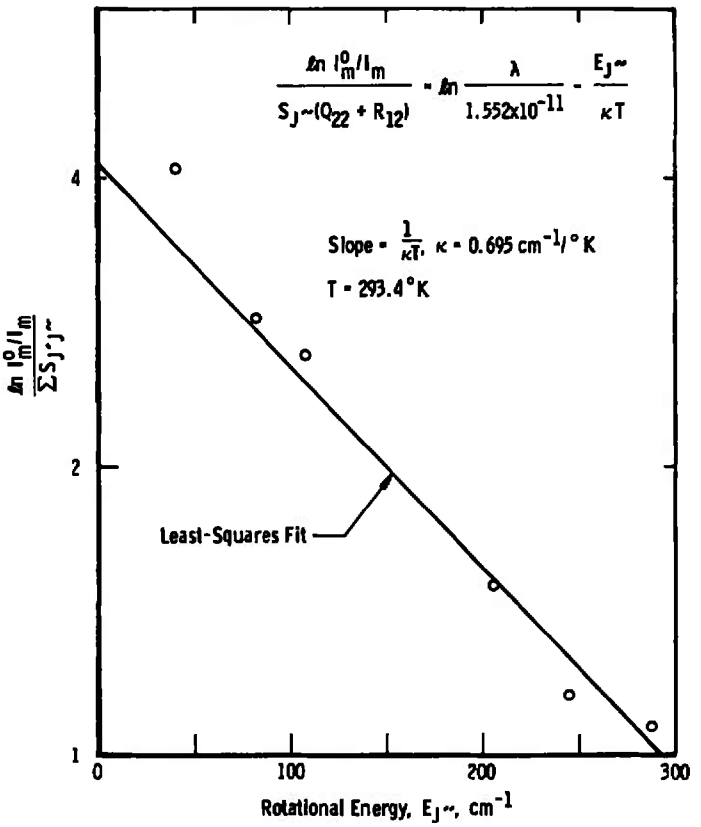


**Fig. 14 Boltzmann Plot of Rotational Line Transmission for Determination of Rotational Temperature**

## 5.2 Discussion of the Method

### 5.2.1 Validity of the Derived Working Equation

The work reported above serves to assemble the necessary analysis and molecular data for the use of measurement of the absorption coefficient of rotational lines in the $\gamma$-system of NO to determine concentration of the NO molecule. Furthermore, the experimental measurement serves to validate the accuracy of the derived working equations, Eqs. (57) and (58). This is gratifying for the following reasons. Derivation of an accurate expression such as Eq. (54) is tedious because of the bookkeeping necessary to keep track of the various statistical weights and partition junctions for rotational states of diatomic molecules. Moreover, the state of normalization of expressions for Hönl-London factors such as those expressed in Table IV (Ref. 7) is always suspect.

Expression of the Boltzmann population densities and line strengths must also be done in a systematic way. The approach taken by Tatum (Ref. 5) was strictly adhered to in this derivation, with apparent success.

### 5.2.2 Use of the Correction for Non-Narrow Line Source

The method for converting the measured transmission to line center transmission, when the source line width is about the same magnitude as the absorber line width, was of great use in this work. The ratio:

$$a = \frac{\Delta\lambda\,(\text{source})}{\Delta\lambda\,(\text{absorber})} \tag{60}$$

may be expressed as

$$a = \sqrt{\frac{T\,(\text{source})}{T\,(\text{absorber})}} \tag{61}$$

when Doppler broadening can be considered the principal broadening mechanism. In the experimental situation encountered in this report, the source temperature was estimated as 393°K while the temperature of the absorbing gas was room temperature (293°K). Then, a = 1.16, the value used in the correction. If the source temperature estimate is wrong by ±20°K, the correction curve shown in Appendix I will not change by an appreciable amount. The theoretical accuracy of the correction cannot be stated with any degree of confidence because of the complexity of the derivation (see Ref. 1). However, as shown by the data in Fig. 13, the correction works rather well.

As the temperature of the absorber gas increases to that typical of combustion gas streams, such as jet engine exhausts (one to three thousand degrees Kelvin), "a" becomes small, and the correction becomes less important. However, for use in the detection of NO in the atmosphere, the correction is necessary.

### 5.2.3 Non-Uniform Absorbing Media

The transmittance depends on the temperature and concentration along the absorbing path. If these are constant along the path, then Eq. (54) is directly applicable for determination of either concentration or temperature. If either temperature or concentration is variable along

the path, then additional knowledge is necessary to deduce profiles from measured transmittances. If the temperature profile is known from some other measurement, then the total number of absorbing molecules along the path can be determined by breaking the path up into any number of zones of constant temperature. If the absorbing gas stream is axisymetric, then the radial profile of both concentration and temperature can be determined by use of the Abel integral inversion technique as reported by Seiber (Ref. 3) and discussed previously. This method requires that several measurements be made through a plane of the axisymetric flow.

### 5.2.4 Range of Application

The concentration range is limited because of experimental constraints to values of $I_o/I_m$ from about 1.05 to 10. This, in turn, limits the range in the product $k_o\ell$ from about 0.07 to 2.3. Since $k_o$ varies as $N_o$, the range of $N_o$ can be controlled somewhat by controlling the path length ($\ell$). Some control over the range is also afforded by choice of the rotational line used, as illustrated in the curves in Fig. 13. For example, the $P_{22}(35/2) + Q_{12}(35/2)$ line can theoretically be used for values of $N_o$ up to about $10^{16}$ $cm^{-3}$ at room temperature, while the $Q_{22}$, $R_{12}$ lines are only useful up to about $3 \times 10^{15}$ $cm^{-3}$. The lower limit for all the useful lines in the (0,0) band of the NO $\gamma$-system is about $10^{14}$ $cm^{-3}$. If the temperature of the absorber is increased to 2000°K then the upper limit is reduced to about $10^{15}$ $cm^{-3}$ for the $P_{22}$, $Q_{22}$ lines but does not change appreciably for the $Q_{22}$, $R_{12}$ lines.

The overall range of NO which can be measured using the absorption technique is mainly controlled by the value

$$f_{v'v''} \exp[-G(v'')/\kappa T]/\sum_{v''} \exp[-G(v'')/\kappa T] \tag{62}$$

in Eq. (54). For $v'' = 0$, the exponentials reduce to unity at room temperature so that, for the (0,0) band, this expression is just $f_{oo}$. However, for $v'' = 1$, $v' = 0$, the expression becomes

$$\frac{f_{o1} \exp[-G(1)/\kappa T]}{\sum_{v} \exp[-G(v'')/\kappa T]} = \frac{q_{o1}}{q_{oo}} f_{oo} \frac{\exp[-2828/(0.695)(293)]}{\exp[-950/(0.695)(293)]} \tag{63}$$

Values of the Franck-Condon factors are given in Ref. 17 and are listed in Table III. The expression has a value of $1.62 \times 10^{-4}$ $f_{oo}$ and therefore, for the (0,1) band,

$$N_o = 4.45 \times 10^{16} \frac{\ln (I_o/I_m)}{L} \frac{1}{\lambda \exp[-E_{J''}/\kappa T] S_{J''}} \tag{64}$$

The measurable range of $N_o$ for lines in the (0,1) band is thus from about $5 \times 10^{17}$ to about $10^{19}$ $cm^{-3}$. Measurements in this range using the (0,1) band were made previously by Litton (Ref. 18).

### 5.2.5 Validity of Oscillator Strengths

After careful evaluation of the experiments reported in the literature, the value of $f_{oo}$ selected for this study was that of Perry-Thorne and Banfield (Ref. 16), which was determined by the Hook interferometric technique. Hasson, Farmer, and Nichols (Ref. 19) have recently published new values obtained by a modification of this technique and have reviewed the values obtained by several investigators using several methods. Their concensus is that the value lies near $4.1 \times 10^{-4}$. The deviation of this value from that of Ref. 16 is $\pm 13$ percent. The experiment carried out in this study would have detected consistent deviations greater than about 5 percent. Thus, it is concluded that the Perry-Thorne and Banfield value was not a bad choice, and that other published values may be somewhat high.

## SECTION VI
## CONCLUSIONS

The following conclusions can be reached from this study:

1. The theoretical approach to spectral line absorption, when details are carefully attended to, leads to accurate expression for the number density of NO in terms of the measured line transmission, molecular properties, and the gas temperature.
2. The oscillator strength reported in the literature by Perry-Thorne and Banfield (Ref. 16) appears to be correct.
3. Application of the correction of measured transmission to transmission at line center, using the method of Mitchel and Zemansky (Ref. 1), is necessary when the temperature of the absorbing gas is not much greater than that of the source, and appears adequate for absorption values not exceeding about 50 percent.

4. The method, as applied here, using the (0,0) $\gamma$-band leads to determinations of NO number density with an uncertainty not exceeding 20 percent for values of $N_o$ between about $10^{14}$ and $3 \times 10^{15}$ $cm^{-3}$, at path lengths of about 50 cm. The range can be adjusted somewhat by choice of spectral line used or the path length. For larger densities, the (0,1), (0,2), etc., bands may also be used.

## REFERENCES


1. Mitchel, A. C. G. and Zemansky, M. W. Resonance Radiation and Excited Atoms. The McMillan Co., New York, 1934.
2. Davis, M. G., McGregor, W. K., and Mason, A. A. "Determination of the Excitation Reaction of the OH Radical in $H_2$-$O_2$ Combustion." AEDC-TR-69-95 (AD695471), Oct. 1969.
3. Seiber, B. L. "Narrow Line OH Absorption Diagnostics of Cylindrically Symmetric Combustion Gas Streams." AEDC-TR-
4. Thorson, W. R. and Badger, R. M. "On the Pressure Broadening in the Gamma Bands of Nitric Oxide." Journal of Chemical Physics, Vol. 27, p. 609, September 1957.
5. Tatum, J. B. "The Interpretation of Intensities in Diatomic Molecular Spectra." The Astrophysical Journal, supplement No. 124, p. 21, March 1967.
6. Schadee, A. "The Relation between the Electronic Oscillator Strength and the Wavelength for Diatomic Molecules." Journal of Quantitative Spectroscopy and Radiative Transfer, Vol. 7, p. 169, 1967.
7. Earls, L. T. "Rotational Strength Factors for $^2\Sigma \rightarrow {}^2\Pi$ Transitions." Physical Review, Vol. 48, p. 423, 1935.
8. Kovacs, L. Rotational Structure in the Spectra of Diatomic Molecules, Adam Hilger Ltd, London, 1969.
9. Gero, L. and Schmid, R. "Dissociation Energy of the NO Molecule." Proceedings of the Physical Society, Vol. 60, p. 533, 1947.

10. Herzberg, G. Spectra of Diatomic Molecules. van Nostrand Co., Inc., New York, 1950.

11. Deezsi, I. "A Recent Rotational Analysis of the $\gamma$-Bands of the NO Molecule." Acta Physica, Vol. 9, p. 125, 1957.

12. Gero, L., Schmid, R., and von Szily, F. K. "Rotations Analyse der E-Banden des NO-Molekuls." Physica, Band 11 p. 144, Maart, 1944.

13. Gillette, R. H. and Eyster, E. H. "The Fundamental Rotation-Vibration Band of Nitric Oxide." Physical Review, Vol. 57, p. 1113, December 1939.

14. Churchill, D. R., Hagstrom, S. A., and Landshoff, R. K. M. "The Spectral Coefficient of Heated Air." The Journal of Quantitative Spectroscopy and Radiative Transfer, Vol. 4, p. 291, 1964.

15. Barrow, R. F. and Miescher, E. "Fine Structure Analysis of NO Absorption Bands in the Schumann Region." Proceedings of the Physical Society, Vol. A70, p. 219, 1957.

16. Perry-Thorne, A. and Banfield, F. P. "Absolute Oscillator Strength of Nitric Oxide by the Hook Method." Journal of Physics B, Atomic and Molecular Physics, Vol. 3, p. 1011, 1970.

17. Spindler, R. J., Isaacson, L., and Wentink, T. "Franck-Condon Factors and r-Centroids for the Gamma System of NO." Journal of Quantitative Spectroscopy and Radiation Transfer, Vol. 10, p. 621, 1970.

18. Litton, C. D. "Development of a Technique for Measuring Nitric Oxide Concentration." M. S. Thesis, The University of Tennessee, June 1971.

19. Hasson, V., Farmer, A. J. D., Nichols, R. W., and Anketell, J. "Oscillator Strength of the (0,0) Band of NO - $\gamma(A\ ^2\Sigma - X\ ^2\Pi)$ System." The Journal of Physics B, Atomic and Molecular Physics, Vol. 5, p. 1248, June 1972.

# APPENDIXES

I. DESCRIPTION OF METHOD FOR CONVERSION OF MEASURED LINE TRANSMISSION TO LINE CENTER TRANSMISSION FOR NON-NARROW LINE SOURCES

II. DESCRIPTION OF COMPUTER SIMULATION AND BAND SPECTRA

# APPENDIX I
# DESCRIPTION OF METHOD FOR CONVERSION OF MEASURED LINE TRANSMISSION TO LINE CENTER TRANSMISSION FOR NON-NARROW LINE SOURCES

The accurate measurement of the absorption coefficient at line center ($k_{\nu_o}$) is the key to the "narrow line absorption method." The ideal case is one in which the line source has a width that is much narrower than the absorption line. In the practical case, this condition is rarely met, but, fortunately, a correction can be made to the measured transmission that adequately compensates for the experimental condition. The basic requirements for the correction are given by Mitchell and Zemansky (Ref. 1).

The general expression for the measured transmission ($t_m$) is

$$t_m = \frac{\int I_\nu \, d\nu}{\int I_\nu^o \, d\nu} \tag{I-1}$$

where $I_\nu^o$ is the incident spectral intensity and $I_\nu$ is the transmitted spectral intensity at a frequency ($\nu$), $I_\nu$ is related to $I_\nu^o$ by

$$I_\nu = I_\nu^o \exp(-k_\nu \ell) \tag{I-2}$$

If the absorption line is subject only to Doppler broadening, then

$$k_\nu = k_{\nu_o} \exp\left\{-\left[2\frac{(\nu - \nu_o)}{\Delta\nu_D}\sqrt{\ln 2}\right]^2\right\} = k_{\nu_o} \exp(-W^2) \tag{I-3}$$

where $k_{\nu_o}$ is the absorption coefficient at the line center frequency ($\nu_o$), $\Delta\nu_D$ is the width of the Doppler profile at half intensity, and W has the obvious definition. Thus

$$I_\nu = I_\nu^o \exp[-k_{\nu_o} \ell \exp(-W^2)] \tag{I-4}$$

Now, let

$$a = \frac{\text{emitter Doppler width}}{\text{absorber Doppler width}}$$

then

$$I_\nu^o = I_{\nu_o}^o \exp[-(W/a)^2] \tag{I-5}$$

Substituting Eqs. (I-4) and (I-5) into Eq. (I-1) gives the transmission:

$$t_m = \frac{\int_0^\infty \exp\left[-(W/a)^2\right] \exp\left\{\left[-k_{\nu_o}\ell\right] \exp\left[-W^2\right]\right\} dW}{\int_0^\infty \exp\left[-(W/a)^2\right] dW} \tag{I-6}$$

As shown in Ref. 1, this expression can be expanded in a series as follows:

$$t_m = 1 - \frac{k_{\nu_o}\ell}{\sqrt{1+a^2}} + \frac{(k_{\nu_o}\ell)^2}{2!\sqrt{1+2a^2}} + \cdots + (-1)^{n-1}\frac{(k_{\nu_o}\ell)^n}{n!\sqrt{1+na^2}} + \cdots \tag{I-7}$$

Equation (I-6), or (I-7), expresses the actual, measured value of the transmission ($t_m$) in terms of the true value of the transmission at the line center ($k_{\nu_o}\ell = \ell n(I_{\nu_o}/I^o_{\nu_o}) = \ell n\ t_{\nu_o}$) through the parameter (a). For Doppler broadening,

$$\Delta\nu_D = 2\nu_o\sqrt{\frac{2\kappa T \ell n 2}{Mc^2}} \tag{I-8}$$

where $\kappa$ is Boltzmann's constant, M is the molecular weight, c is the velocity of light, and T is the temperature, so that

$$a = \sqrt{\frac{T(\text{source})}{T(\text{absorber})}} \tag{I-9}$$

Equation (I-6) can be evaluated numerically to give $t_m$ as a function of $\nu_o$ with "a" as a parameter.

In Fig. (I-1) is plotted $t_m^{-1}$ versus $t_{\nu_o}^{-1}$ for several values of "a" ranging from 0 to 1.5. The particular value of a = 1.16 applies to the condition of a 110°C source temperature being transmitted through a room temperature (20°C) absorber. For example, at this condition, a measured value of $t_m^{-1} = 2$ when corrected for a = 1.16 becomes $t_{\nu_o}$ = 3.15; that is, the measured 50-percent transmission would be 32-percent transmission if a = 0, the condition of a very narrow emission line.

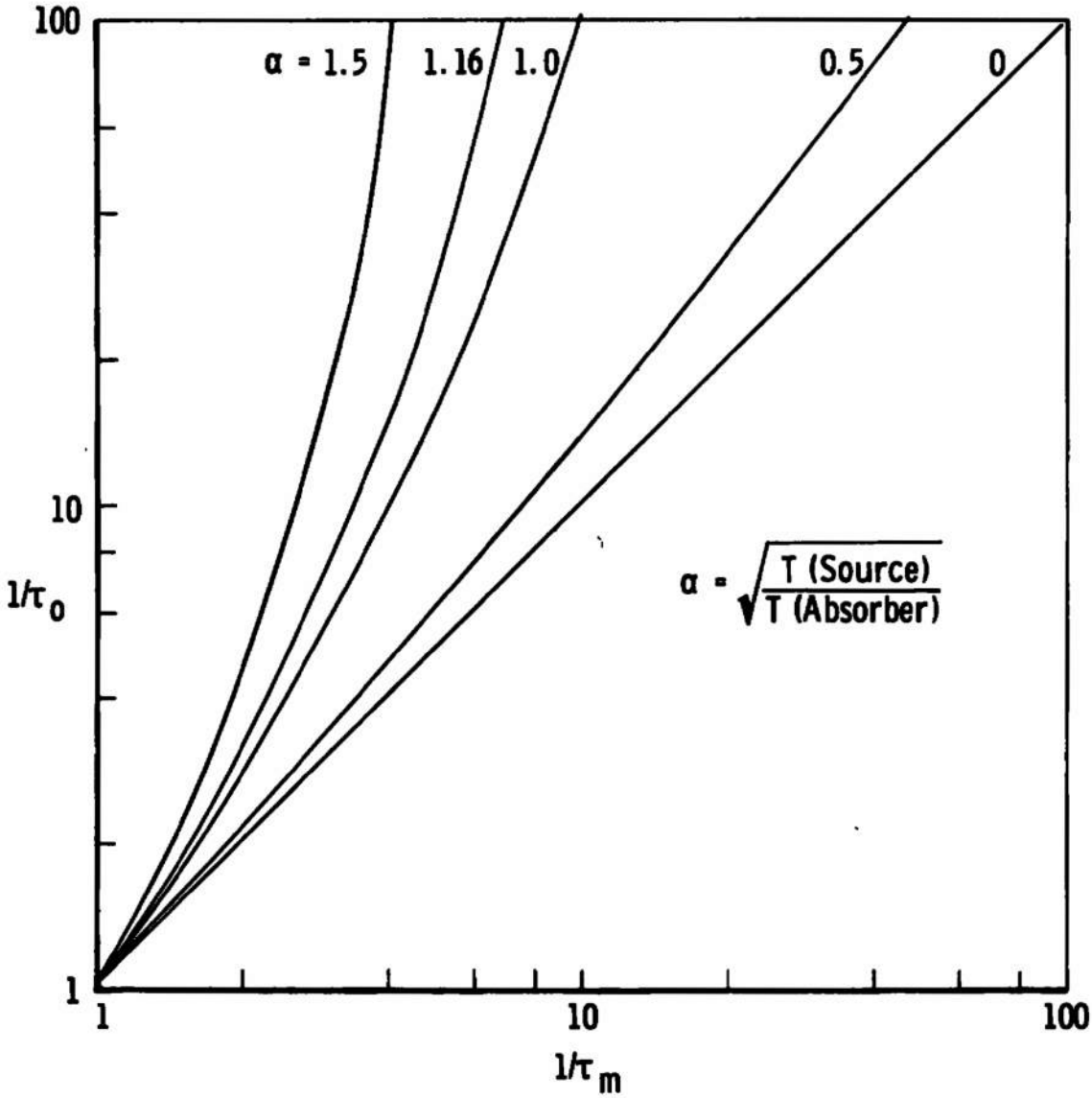


Fig. I-1 Conversion of Measured Transmission at Line Center for Doppler Broadened Lines (Ref. 1)

# APPENDIX II
# DESCRIPTION OF COMPUTER SIMULATION AND BAND SPECTRA

A computer program and plotting procedure for computing and simulating the rotational structure of vibrational bands in electronic transitions of diatomic molecules is described in this appendix. The program proceeds to compute and print out the energy levels in $cm^{-1}$ for the upper and lower states selected for the transition, using the standard equations (Ref. 10):

$$\underline{\text{Upper}} \quad \mathcal{T}' = \mathcal{T}_e' + G'(v') + F_n'(J') \tag{II-1}$$

$$\underline{\text{Lower}} \quad \mathcal{T}'' = \mathcal{T}_e'' + G''(v'') + F_n''(J'') \tag{II-2}$$

where

$\mathcal{T}$ – total energy of the state

$\mathcal{T}_e$ – electronic state energy at $v = 0, J = 0$

$G(v)$ – vibrational energy of the $v = 0, 1, 2, 3 \cdots$ vibrational state

$F_n(J)$ – rotational energy of the $J = 0, 1, 2, \cdots$ rotational state for multiplet states, $n = 1, 2, 3, \cdots$ so that $\mathcal{T}$ has a different value for each multiplet

The standard equation is used throughout for the vibrational energy:

$$G(v) = \omega_e(v + 1/2) - \omega_e x_e(v + 1/2)^2 + \omega_e y_e(v + 1/2)^2, \; v = 0, 1, 2 \cdots \tag{II-3}$$

The quantities $\omega_e$, $\omega_e x_e$, and $\omega_e y_e$ are vibrational constants of the molecule which may generally be found in Herzberg (Ref. 10) or in the published literature. In special cases, the constants may be different for the different components of a multiplet.

The expression ($F_n$) for the rotational energy term is usually different for each molecule and is considered as an input to the program. All $\Sigma$ states belong to Hund's coupling case "b" (Ref. 10), and for $^2\Sigma$ states (the upper state for the NO $\gamma$-band system is a $^2\Sigma$ state), the equations are

$$F_1(J') = B_v(J' + 1/2)(J' - 1/2) + 1/2\Gamma(J' - 1/2) - D_v(J' + 1/2)^2(J' - 1/2)^2$$
$$J' = 1/2, 3/2, 5/2, \cdots \tag{II-4a}$$

$$F_2(J') = B_v(J'+1/2)(J'+3/2) - 1/2\Gamma(J'+3/2) - D_v(J'+1/2)^2(J'+3/2)^2$$
$$J' = 1/2, 3/2, 5/2, \cdots \qquad \text{(II-4b)}$$

The rotational constants $B_v$ and $D_v$ depend on v and are given by

$$B_v = B_e - \alpha_e(v + 1/2) \qquad \text{(II-5)}$$

$$D_v = D_e + \beta_e(v + 1/2) \qquad \text{(II-6)}$$

with $B_e$, $\alpha_e$, $D_e$, and $\beta_e$ constant. The constant $\Gamma$ is known as the spin splitting constant and is usually very small for $\Sigma$ states. The lower rotational state of NO is a $^2\Pi$ state intermediate between Hund's cases "a" and "b" and for such a case the Hill and van Fleck formula was derived (Ref. 10). It is expressed as follows:

$$F_1(J'') = B_v[(J''+1/2)^2 - 1 - u] - D_vJ''^4 \qquad \text{(II-7a)}$$

$$F_2(J'') = B_v[(J''+1/2)^2 - 1 + u] - D_v(J''+1)^4 \qquad \text{(II-7b)}$$

where $B_v$ and $D_v$ are expressed as in Eqs. (II-5) and (II-6) and u is given by

$$u = [(J''+1/2)^2 - Y_v(1 - Y_v/4)]^{1/2} \quad \text{(II-8)} \qquad \text{(II-8)}$$

with $Y_v = A/B_v$, A being the coupling constant.

The constants for NO used in these calculations were the most accurate available; for the X $^2\Pi$ state, the values of Gillette and Eyster (Ref. 13) were used, and for the A $^2\Sigma$ state, those obtained by Barrow and Miescher (Ref. 15) were used. The term values are given for J values out to 81/2 for the v = 0 and v = 1 vibrational states in Table II-1.

The spectral line computations are made in the program from the equation:

$$\nu = \frac{1}{\lambda} = \mathcal{T}' - \mathcal{T}'' \text{ cm}^{-1}$$
$$= (\mathcal{T}_e' - \mathcal{T}_e'') + [G(v') - G(v'')] + [F_n(J') - F_n(J'')] \qquad \text{(II-9)}$$
$$\Delta v = 0, \pm 1, \pm 2, \cdots$$

$$\Delta J = \begin{cases} +1 & \text{R branches} \\ 0 & \text{Q branches} \\ -1 & \text{P branches} \end{cases}$$

Each kind of transition, $^2\Sigma \rightarrow {}^2\Pi$, $^3\Sigma \rightarrow {}^3\Pi$, $^1\Delta \rightarrow {}^1\Sigma$, etc., has its own peruliarities (Q formed P branches, R formed Q branches, etc.) which are described adequately by Herzberg (Ref. 10). Suffice it to say here that the computer programming problem in computing these spectral line wavelengths is mainly one of tedious bookkeeping. For the NO molecule, all 12 possible doublet-to-doublet transitions are present, and the details of the structure are explained in the text of this report. The computed spectra ($\nu$ and $\lambda$) are given in Table II-2 for all the branches of the (0,0) band.

Two methods of plotting the spectra are available. First, the lines of the different branches of a single band may be separated and then combined as shown in Fig. 5 of the text. This plot is similar to what would be observed on a photographic plate from a spectrograph and permits identification of the individual lines. It is of especial value in determining which lines overlap in a spectrum of given resolving power.

In the second method of plotting, an attempt is made to simulate the spectrum that would be produced by a monochrometer. For this purpose, it is also necessary to compute the intensities of the lines. Most sources produce spectra that exhibit near-Boltzmann-like distributions in rotational line distribution with some less-Boltzmann-like vibrational distributions. For purposes of comparison of computed spectra to real spectra, the assumption of a Boltzmann distribution was made. Then, the emission coefficient ($\epsilon_{J'J''}$) of the rotational lines within a band are given by

$$\epsilon_{J'J''} = \frac{hc}{\lambda_{J'J''}} A_{n'n''} q_{v'v''} \frac{\delta_{J'J''}}{(2J'+1)g_{n'}} \qquad \text{(II-10)}$$

where

$h$ = Plank's constant, erg sec

$c$ = velocity of light, cm/sec

$\lambda_{J'J''}$ = wavelength of the spectral line produced by the $J' - J''$ transition, cm

$q_{v'v''}$ = vibrational overlap integral, or Franck-Condon factor (Ref. 10)

$\delta_{J'J''}$ = rotational strength, or Hönl-London factor for the rotational transition

$2S' + 1$ = statistical weight of the rotational level

$g_{n'}$ = statistical weight of the electronic level; equal to $(2S + 1)$ for $\Sigma$ states or $2(2S + 1)$ for other states

$N(n', v', J')$ = number of molecules occupying the $J'$ rotational state in the $v'$ vibrational level of the $n'$ electronic level

For the Boltzmann distribution, the distribution of vibrational and rotational states within the electronic level is given by

$$N(v', J') = N_o \frac{\exp[-G(v')/\kappa T]}{\sum_{v'} \exp[-G(v')/\kappa T]} \times \frac{g_{J'} \exp[(-F_n J')/\kappa T]}{\sum_{J'} g_{J'} \exp[(-F_n G v')/\kappa T]} \qquad \text{(II-11)}$$

where:

$N_o$ = total number of molecules

$\kappa$ = Boltzmann's constant, 0.6952 $cm^{-1}/°K$

T = Temperature (II-12)

$g_{J'}$ = statistical weight of the rotational state; usually

$g_{J'}$ = $(2S + 1)(2J'' + 1)$, $\Sigma$ states
$2(2S + 1)(2J' + 1)$, other states

(See Ref. 5 for exceptions to this expression.) The computation of the intensity of each line proceeds from Eqs. (II-10) and (II-11). The values of $A_{n'n''}$ and $q_{v'v''}$ are found in the literature for most bands. If the interest is only in the rotational distribution with a band, then the product of all the terms not explicitly dependent on $J'$ may be set to unity. This is done in the present report. Or, the entire equation may be utilized if all the terms are known.

The quantity $\delta_{J'J''}$ must be given special attention, since, for other than singlet transitions, it may become quite involved. Expressions for $\delta_{J'J''}$ like F(J) are usually different for each case computed and depend on the electronic momentum states and the degree of coupling of orbital, spin, and rotational angular momentum as expressed by Hund's coupling cases. For the $^2\Sigma \rightarrow {}^2\Pi$ transition with the $^2\Pi$ state intermediate between Hund's cases "a" and "b" (the case for NO $\gamma$-bands), the formulas of Table IV are used. In the computer program the expression for $_{J'J''}$ is input for each spectra to be calculated.

The simulation of the monochrometer as usually recorded on a strip chart recorder is accomplished by numerical integration of the components of each line as determined by the wavelength, the line strength, the line width, and the monochrometer bandpass. The line width consideration will not be a part of this Appendix because the line broadening (natural, pressure, Doppler, Stark) encountered in this study are much smaller than the bandpass of the instrument used. However, the computer program is capable of handling these phenomena. The instrument band pass is taken here as a triangular function:

$$\int \epsilon_\lambda d\lambda \epsilon = \epsilon_0 \begin{cases} \dfrac{\Delta\lambda - (\lambda_0 - \lambda)}{\Delta\lambda}, \lambda < \lambda_0; 0, \lambda < \lambda_0 - \Delta\lambda \\ \dfrac{\Delta\lambda - (\lambda - \lambda_0)}{\Delta\lambda}, \lambda > \lambda_0; 0, \lambda > \lambda_0 + \Delta\lambda \end{cases} \tag{II-13}$$

where $\epsilon_0$ is the emission coefficient as computed in Eq. (II-10), $\lambda_0$ is the wavelength at the center of the line, and $\Delta\lambda$ is the half-width of the triangular bandpass. The equivalent half-width in wavelength units is given by the product of the reciprocal dispersion (Å/mm) of the instrument and the actual instrument slit width in mm (assuming entrance and exit slit widths are equal as in the case for all work reported here). The computer is then given a temperature, $\Delta\lambda$, the molecule constants, and a wavelength plotting scale (Å per inch of recording paper) which is the same as the experimental scale. Simulated spectra for the (0,0) band of the NO $\gamma$-system then appear as in Fig. 6. If the overlap of lines within an apparent peak is suspected, then $\Delta\lambda$ may be set equal to zero, and the spectrum as plotted in Fig. 6 results.

This computer program is of great utility in studies of the nature of this report, and line identification from experimental data is almost impossible without it. The program is written for the IBM-370/155 computer with a Cal-Comp plotter.

# TABLE II-1
# TERM VALUES FOR THE $A^2\Sigma$ AND THE $X^2\Pi$ STATES OF NO IN WAVE NUMBERS

### $v'' = 0$, $X\,^2\Pi$ State

| | $F_1(J'')$ | $F_2(J'')$ |
|---|---|---|
| J= 0.5 | -9.503528E 02 | -1.070851E 03 |
| J= 1.5 | -9.553684E 02 | -1.076010E 03 |
| J= 2.5 | -9.637283E 02 | -1.084607E 03 |
| J= 3.5 | -9.754321E 02 | -1.096643E 03 |
| J= 4.5 | -9.904810E 02 | -1.112114E 03 |
| J= 5.5 | -1.008874E 03 | -1.131028E 03 |
| J= 6.5 | -1.030614E 03 | -1.153378E 03 |
| J= 7.5 | -1.055700E 03 | -1.179162E 03 |
| J= 8.5 | -1.084134E 03 | -1.208382E 03 |
| J= 9.5 | -1.115915E 03 | -1.241037E 03 |
| J=10.5 | -1.151045E 03 | -1.277127E 03 |
| J=11.5 | -1.189525E 03 | -1.316649E 03 |
| J=12.5 | -1.231356E 03 | -1.359603E 03 |
| J=13.5 | -1.276539E 03 | -1.405988E 03 |
| J=14.5 | -1.325074E 03 | -1.455802E 03 |
| J=15.5 | -1.376966E 03 | -1.509046E 03 |
| J=16.5 | -1.432209E 03 | -1.565717E 03 |
| J=17.5 | -1.490811E 03 | -1.625816E 03 |
| J=18.5 | -1.552770E 03 | -1.689337E 03 |
| J=19.5 | -1.618088E 03 | -1.756284E 03 |
| J=20.5 | -1.686765E 03 | -1.826653E 03 |
| J=21.5 | -1.758804E 03 | -1.900445E 03 |
| J=22.5 | -1.834205E 03 | -1.977657E 03 |
| J=23.5 | -1.912968E 03 | -2.058289E 03 |
| J=24.5 | -1.995096E 03 | -2.142339E 03 |
| J=25.5 | -2.080590E 03 | -2.229807E 03 |
| J=26.5 | -2.169449E 03 | -2.320691E 03 |
| J=27.5 | -2.261677E 03 | -2.414991E 03 |
| J=28.5 | -2.357272E 03 | -2.512706E 03 |
| J=29.5 | -2.456236E 03 | -2.613833E 03 |
| J=30.5 | -2.558571E 03 | -2.718374E 03 |
| J=31.5 | -2.664276E 03 | -2.826327E 03 |
| J=32.5 | -2.773354E 03 | -2.937690E 03 |
| J=33.5 | -2.885803E 03 | -3.052464E 03 |
| J=34.5 | -3.001627E 03 | -3.170647E 03 |
| J=35.5 | -3.120824E 03 | -3.292239E 03 |
| J=36.5 | -3.243397E 03 | -3.417238E 03 |
| J=37.5 | -3.369344E 03 | -3.545646E 03 |
| J=38.5 | -3.498668E 03 | -3.677459E 03 |
| J=39.5 | -3.631369E 03 | -3.812679E 03 |
| J=40.5 | -3.767447E 03 | -3.951304E 03 |

### $v' = 0$, $A\,^2\Sigma$ State

| | $F_1(J'')$ | $F_2(J'')$ |
|---|---|---|
| J= 0.5 | 4.514898E 04 | 4.515296E 04 |
| J= 1.5 | 4.515296E 04 | 4.516091E 04 |
| J= 2.5 | 4.516091E 04 | 4.517284E 04 |
| J= 3.5 | 4.517284E 04 | 4.518874E 04 |
| J= 4.5 | 4.518874E 04 | 4.520862E 04 |
| J= 5.5 | 4.520862E 04 | 4.523247E 04 |
| J= 6.5 | 4.523247E 04 | 4.526030E 04 |
| J= 7.5 | 4.526030E 04 | 4.529211E 04 |
| J= 8.5 | 4.529211E 04 | 4.532788E 04 |
| J= 9.5 | 4.532788E 04 | 4.536764E 04 |
| J=10.5 | 4.536764E 04 | 4.541137E 04 |
| J=11.5 | 4.541137E 04 | 4.545908E 04 |
| J=12.5 | 4.545908E 04 | 4.551076E 04 |
| J=13.5 | 4.551076E 04 | 4.556642E 04 |
| J=14.5 | 4.556642E 04 | 4.562605E 04 |
| J=15.5 | 4.562605E 04 | 4.568966E 04 |
| J=16.5 | 4.568966E 04 | 4.575725E 04 |
| J=17.5 | 4.575725E 04 | 4.582881E 04 |
| J=18.5 | 4.582881E 04 | 4.590435E 04 |
| J=19.5 | 4.590435E 04 | 4.598386E 04 |
| J=20.5 | 4.598386E 04 | 4.606734E 04 |
| J=21.5 | 4.606734E 04 | 4.615481E 04 |
| J=22.5 | 4.615481E 04 | 4.624625E 04 |
| J=23.5 | 4.624625E 04 | 4.634166E 04 |
| J=24.5 | 4.634166E 04 | 4.644105E 04 |
| J=25.5 | 4.644105E 04 | 4.654442E 04 |
| J=26.5 | 4.654442E 04 | 4.665176E 04 |
| J=27.5 | 4.665176E 04 | 4.676307E 04 |
| J=28.5 | 4.676307E 04 | 4.687837E 04 |
| J=29.5 | 4.687837E 04 | 4.699764E 04 |
| J=30.5 | 4.699764E 04 | 4.712088E 04 |
| J=31.5 | 4.712088E 04 | 4.724810E 04 |
| J=32.5 | 4.724810E 04 | 4.737929E 04 |
| J=33.5 | 4.737929E 04 | 4.751446E 04 |
| J=34.5 | 4.751446E 04 | 4.765361E 04 |
| J=35.5 | 4.765361E 04 | 4.779673E 04 |
| J=36.5 | 4.779673E 04 | 4.794383E 04 |
| J=37.5 | 4.794383E 04 | 4.809490E 04 |
| J=38.5 | 4.809490E 04 | 4.824995E 04 |
| J=39.5 | 4.824995E 04 | 4.840897E 04 |
| J=40.5 | 4.840897E 04 | 4.857197E 04 |

### $v'' = 1$, $X\,^2\Pi$ State

| | $F_1(J'')$ | $F_2(J'')$ |
|---|---|---|
| J= 0.5 | -2.826695E 03 | -2.946809E 03 |
| J= 1.5 | -2.831659E 03 | -2.951713E 03 |
| J= 2.5 | -2.839932E 03 | -2.960218E 03 |
| J= 3.5 | -2.851515E 03 | -2.972124E 03 |
| J= 4.5 | -2.866408E 03 | -2.987435E 03 |
| J= 5.5 | -2.884611E 03 | -3.006146E 03 |
| J= 6.5 | -2.906126E 03 | -3.028256E 03 |
| J= 7.5 | -2.930952E 03 | -3.053767E 03 |
| J= 8.5 | -2.959091E 03 | -3.082677E 03 |
| J= 9.5 | -2.990543E 03 | -3.114985E 03 |
| J=10.5 | -3.025309E 03 | -3.150691E 03 |
| J=11.5 | -3.063390E 03 | -3.189793E 03 |
| J=12.5 | -3.104787E 03 | -3.232291E 03 |
| J=13.5 | -3.149501E 03 | -3.278183E 03 |
| J=14.5 | -3.197533E 03 | -3.327469E 03 |
| J=15.5 | -3.248885E 03 | -3.380148E 03 |
| J=16.5 | -3.303556E 03 | -3.436217E 03 |
| J=17.5 | -3.361549E 03 | -3.495677E 03 |
| J=18.5 | -3.422865E 03 | -3.558526E 03 |
| J=19.5 | -3.487503E 03 | -3.624764E 03 |
| J=20.5 | -3.555467E 03 | -3.694388E 03 |
| J=21.5 | -3.626756E 03 | -3.767398E 03 |
| J=22.5 | -3.701372E 03 | -3.843793E 03 |
| J=23.5 | -3.779316E 03 | -3.923571E 03 |
| J=24.5 | -3.860589E 03 | -4.006732E 03 |
| J=25.5 | -3.945193E 03 | -4.093275E 03 |
| J=26.5 | -4.033126E 03 | -4.183195E 03 |
| J=27.5 | -4.124391E 03 | -4.276500E 03 |
| J=28.5 | -4.218988E 03 | -4.373180E 03 |
| J=29.5 | -4.316922E 03 | -4.473242E 03 |
| J=30.5 | -4.418186E 03 | -4.576676E 03 |
| J=31.5 | -4.522793E 03 | -4.683488E 03 |
| J=32.5 | -4.630730E 03 | -4.793680E 03 |
| J=33.5 | -4.742005E 03 | -4.907246E 03 |
| J=34.5 | -4.856621E 03 | -5.024176E 03 |
| J=35.5 | -4.974574E 03 | -5.144488E 03 |
| J=36.5 | -5.095867E 03 | -5.268168E 03 |
| J=37.5 | -5.220496E 03 | -5.395219E 03 |
| J=38.5 | -5.348469E 03 | -5.525645E 03 |
| J=39.5 | -5.479785E 03 | -5.659436E 03 |
| J=40.5 | -5.614441E 03 | -5.796602E 03 |

### $v' = 1$, $A\,^2\Sigma$ State

| | $F_1(J'')$ | $F_2(J'')$ |
|---|---|---|
| J= 0.5 | 4.749086E 04 | 4.749480E 04 |
| J= 1.5 | 4.749480E 04 | 4.750267E 04 |
| J= 2.5 | 4.750267E 04 | 4.751448E 04 |
| J= 3.5 | 4.751448E 04 | 4.753022E 04 |
| J= 4.5 | 4.753022E 04 | 4.754990E 04 |
| J= 5.5 | 4.754990E 04 | 4.757352E 04 |
| J= 6.5 | 4.757352E 04 | 4.760107E 04 |
| J= 7.5 | 4.760107E 04 | 4.763256E 04 |
| J= 8.5 | 4.763256E 04 | 4.766798E 04 |
| J= 9.5 | 4.766798E 04 | 4.770734E 04 |
| J=10.5 | 4.770734E 04 | 4.775064E 04 |
| J=11.5 | 4.775064E 04 | 4.779787E 04 |
| J=12.5 | 4.779787E 04 | 4.784904E 04 |
| J=13.5 | 4.784904E 04 | 4.790414E 04 |
| J=14.5 | 4.790414E 04 | 4.796318E 04 |
| J=15.5 | 4.796318E 04 | 4.802616E 04 |
| J=16.5 | 4.802616E 04 | 4.809307E 04 |
| J=17.5 | 4.809307E 04 | 4.816392E 04 |
| J=18.5 | 4.816392E 04 | 4.823870E 04 |
| J=19.5 | 4.823870E 04 | 4.831742E 04 |
| J=20.5 | 4.831742E 04 | 4.840008E 04 |
| J=21.5 | 4.840008E 04 | 4.848667E 04 |
| J=22.5 | 4.848667E 04 | 4.857720E 04 |
| J=23.5 | 4.857720E 04 | 4.867166E 04 |
| J=24.5 | 4.867166E 04 | 4.877006E 04 |
| J=25.5 | 4.877006E 04 | 4.887240E 04 |
| J=26.5 | 4.887240E 04 | 4.897867E 04 |
| J=27.5 | 4.897867E 04 | 4.908888E 04 |
| J=28.5 | 4.908888E 04 | 4.920302E 04 |
| J=29.5 | 4.920302E 04 | 4.932110E 04 |
| J=30.5 | 4.932110E 04 | 4.944312E 04 |
| J=31.5 | 4.944312E 04 | 4.956907E 04 |
| J=32.5 | 4.956907E 04 | 4.969896E 04 |
| J=33.5 | 4.969896E 04 | 4.983278E 04 |
| J=34.5 | 4.983278E 04 | 4.997054E 04 |
| J=35.5 | 4.997054E 04 | 5.011224E 04 |
| J=36.5 | 5.011224E 04 | 5.025787E 04 |
| J=37.5 | 5.025787E 04 | 5.040744E 04 |
| J=38.5 | 5.040744E 04 | 5.056094E 04 |
| J=39.5 | 5.056094E 04 | 5.071838E 04 |
| J=40.5 | 5.071838E 04 | 5.087976E 04 |

# TABLE II-2
## FREQUENCY (cm$^{-1}$) (a), WAVELENGTH (Å) (b), AND HÖNL-LONDON FACTORS (c) FOR ROTATIONAL LINES OF THE (0,0) GAMMA BAND OF NO

V'= 0 V"= 6

P BRANCH

| | 11 | 12 | 21 | 22 |
|---|---|---|---|---|
| J"= 1.5<br>J'= 0 5 | 44193 81 (a)<br>2282 77 (b)<br>0 402 (c) | 44072 97<br>2266 86<br>1 848 | 44197 59<br>2262 57<br>0 530 | 44076 85<br>2266 76<br>1 900 |
| J"= 2 5<br>J'= 1 5 | 44189.23<br>2262.99<br>1 631 | 44068 55<br>2269 20<br>2 094 | 44197 18<br>2262 59<br>0.647 | 44076 50<br>2266 79<br>2 276 |
| J"= 3 5<br>J = 2 5 | 44185 46<br>2263 19<br>1.845 | 44064.27<br>2269 41<br>2 459 | 44197 40<br>2262 58<br>1 278 | 44076 19<br>2268.86<br>2 805 |
| J"= 4 5<br>J'= 3.5 | 44182 55<br>2245 35<br>2 275 | 44060.72<br>2269 60<br>2 788 | 44198 25<br>2262 55<br>1 672 | 44076 62<br>2268 78<br>5 591 |
| J"= 5 5<br>J'= 4.5 | 44179.86<br>2263 47<br>2.928 | 44057 71<br>2269.75<br>5 122 | 44199.74<br>2262.46<br>2 035 | 44077 59<br>2268 75<br>4 015 |
| J"= 6.5<br>J'= 5.5 | 44176.00<br>2263.57<br>5 605 | 44055 24<br>2269 68<br>5 457 | 44201.65<br>2262 55<br>2 571 | 44079 09<br>2268 65<br>4.870 |
| J"= 7.5<br>J'= 6 5 | 44176 77<br>2265 65<br>4.307 | 44055.50<br>2269 98<br>2 729 | 44204 60<br>2262 21<br>2 861 | 44081 14<br>2268 54<br>5.555 |
| J"= 8 5<br>J'= 7.5 | 44176.16<br>2263.66<br>5 022 | 44051.92<br>2270.65<br>3 999 | 44207.97<br>2262 04<br>2 966 | 44085.72<br>2268.41<br>6 065 |
| J"= 9.5<br>J'= 8.5 | 44176 18<br>2262.66<br>5 781 | 44051 07<br>2270.09<br>4 247 | 44211 96<br>2261.63<br>3 227 | 44086 84<br>2266 25<br>8 801 |
| J"=16 5<br>J'= 9 5 | 44176 84<br>2265.63<br>8 555 | 44050 75<br>2270 11<br>4 472 | 44218 59<br>2261 39<br>3 465 | 44090 51<br>2266.06<br>7 580 |
| J"=11.5<br>J'=10 5 | 44178 11<br>2265.56<br>7.546 | 44650 99<br>2270 10<br>4.877 | 44221 84<br>2261 35<br>5 682 | 44094.72<br>2267 85<br>6 341 |
| J"=12.5<br>J'=11.5 | 44186 01<br>2263.47<br>6.160 | 44651 77<br>2270.08<br>4 861 | 44227 72<br>2261 03<br>3 676 | 44099.47<br>2267 60<br>9 143 |
| J"=12.5<br>J'=12.5 | 44162 54<br>2263 34<br>6 994 | 44055.08<br>2289 99<br>5 025 | 44234.22<br>2260.69<br>4 055 | 44104 77<br>2267.55<br>9 985 |
| J"=14 5<br>J'=13 5 | 44165 89<br>2265 18<br>9 646 | 44054 98<br>2269 69<br>5 172 | 44241 35<br>2260 33<br>4 215 | 44110 62<br>2267 05<br>10.805 |
| J"=15 5<br>J'=14 5 | 44169.49<br>2262.98<br>16.716 | 44057 38<br>2268.77<br>6.301 | 44249 09<br>2259 95<br>4 554 | 44117 61<br>2266.70<br>11 663 |
| J"=16 5<br>J'=15 5 | 44195 84<br>2262 78<br>11 862 | 44060.34<br>2269.81<br>5.414 | 44257.45<br>2259.51<br>4.479 | 44123 85<br>2266 34<br>12.557 |
| J"=17 5<br>J'=16.5 | 44186.85<br>2262 50<br>12.503 | 44062.85<br>2269.45<br>5.512 | 44266 44<br>2259 05<br>4.586 | 44151.43<br>2265.96<br>15.427 |
| J"=18 5<br>J'=17 5 | 44204 46<br>2262.21<br>12.418 | 44667.91<br>2269.22<br>5.595 | 44276 04<br>2258 56<br>4.684 | 44139.47<br>2265 55<br>14.336 |
| J"=19 5<br>J'=18.5 | 44210 72<br>2261 69<br>14 347 | 44072 52<br>2268 99<br>5 666 | 44286 26<br>2258.04<br>4 766 | 44148.06<br>2265.10<br>15.247 |
| J"=20 5<br>J'=19.5 | 44217 58<br>2261.54<br>15 289 | 44077.69<br>2268 72<br>5.724 | 44297 09<br>2257.48<br>4 858 | 44157 20<br>2264 64<br>18.177 |
| J"=21.5<br>J'=26.5 | 44225.05<br>2261 16<br>18.241 | 44085.41<br>2268.43<br>5 771 | 44506 54<br>2256 96<br>4 895 | 44166.80<br>2264 14<br>17.117 |
| J"=22 5<br>J'=21 5 | 44253.14<br>2266.75<br>17.204 | 44089.68<br>2268.10<br>5.808 | 44520 60<br>2256.29<br>4 645 | 44177 15<br>2263 61<br>16 068 |

V'= 0 V"= 0

P BRANCH

| | 11 | 12 | 21 | 22 |
|---|---|---|---|---|
| J"=25 5<br>J'=22 5 | 44241 84<br>2260.30<br>16 176 | 44096 52<br>2267.75<br>5 625 | 44333.28<br>2255.64<br>4.962 | 44197 98<br>2263.06<br>19 029 |
| J"=24 5<br>J'=23.5 | 44251 15<br>2259 83<br>19 158 | 44102.91<br>2267 37<br>5 852 | 44346.58<br>2254.97<br>5.012 | 44199 52<br>2262 48<br>19 996 |
| J"=25 5<br>J'=24.5 | 44261 07<br>2259 32<br>20 147 | 44111 85<br>2266 98<br>5.863 | 44560 48<br>2254.26<br>5 034 | 44211 24<br>2261.87<br>20 976 |
| J"=26 5<br>J'=25 5 | 44271 60<br>2258 78<br>21 145 | 44120.36<br>2266 55<br>5.867 | 44374 96<br>2255 52<br>5.049 | 44225 75<br>2261 25<br>21 961 |
| J"=27 5<br>J'=26 5 | 44282 74<br>2258 22<br>22 146 | 44129 45<br>2266 06<br>5 665 | 44590 08<br>2252 76<br>5 057 | 44236 77<br>2260 56<br>22 952 |
| J"=28 5<br>J'=27 5 | 44294 48<br>2257 62<br>25 155 | 44159 05<br>2265 57<br>5 654 | 44405 60<br>2251.96<br>5 059 | 44250 27<br>2259.87<br>23.950 |
| J"=29 5<br>J'=28 5 | 44306 84<br>2256 99<br>24.169 | 44149.24<br>2265 04<br>5 839 | 44422.13<br>2251 13<br>5.058 | 44264.55<br>2259 15<br>24.953 |
| J"=20 5<br>J'=29 5 | 44581.79<br>2256 52<br>25 189 | 44159.99<br>2264 49<br>5 820 | 44459 06<br>2250 27<br>5.048 | 44279.26<br>2258.59<br>25.981 |
| J"=51 5<br>J'=30.5 | 44335 28<br>2255.64<br>26.212 | 44171.21<br>2263.91<br>5.796 | 44458 60<br>2249.56<br>5 635 | 44294.55<br>2257 81<br>26 972 |
| J"=52 5<br>J'=51.5 | 44547.52<br>2254 92<br>27 239 | 44163.18<br>2263.56<br>5.768 | 44474 74<br>2246 47<br>5.018 | 44510 41<br>2258 61<br>27.990 |
| J"=35 5<br>J'=22.5 | 44562 29<br>2254.17<br>28.276 | 44195.63<br>2262.67<br>5.757 | 44493 49<br>2247.52<br>4 998 | 44326.65<br>2255 97<br>29 010 |
| J"=34 5<br>J'=55 5 | 44377 66<br>2253.38<br>29.364 | 44206.64<br>2262 00<br>5 705 | 44512 84<br>2246.54<br>4.975 | 44343 62<br>2255.11<br>30.025 |
| J"=35.5<br>J'=54 5 | 44595.64<br>2252.57<br>30 340 | 44222 22<br>2281 31<br>5.667 | 44522.79<br>2245 54<br>4.946 | 44361.37<br>2254.21<br>31 050 |
| J"=36 5<br>J'=35 5 | 44410.21<br>2251.73<br>31 579 | 44258 37<br>2260.66<br>5.828 | 44553.35<br>2244 50<br>4 920 | 44379 49<br>2253.29<br>32.087 |
| J"=27 5<br>J'=56 5 | 44427 28<br>2250.86<br>22.420 | 44251 08<br>2259 83<br>5 587 | 44574.46<br>2243 44<br>4 689 | 44398 18<br>2252.54<br>52.116 |
| J"=26 5<br>J'=37.5 | 44445.16<br>2249.98<br>55.462 | 44288 37<br>2259.06<br>5.544 | 44598 25<br>2242.34<br>4.836 | 44417.44<br>2251.27<br>34.151 |
| J"=39 5<br>J'=26.5 | 44463.53<br>2249 03<br>34 507 | 44282.22<br>2258 24<br>5.500 | 44618.58<br>2241 22<br>4 821 | 44437 27<br>2250.56<br>35.165 |
| J"=40.5<br>J'=59.5 | 44482.50<br>2246.67<br>35.552 | 44296 64<br>2257.41<br>5.454 | 44641 52<br>2246.07<br>4.788 | 44457.67<br>2249.52<br>36.221 |

# TABLE II-2 (Continued)

V' = 0 V" = 0

Q BRANCH

| | 11 | 12 | 21 | 22 |
|---|---|---|---|---|
| J"= 0 5<br>J'= 0 5 | 44198 82<br>2262.31<br>0.000 | 44078.13<br>2268 70<br>0.000 | 44202.80<br>2262 31<br>0.000 | 44062 11<br>2268.49<br>0.000 |
| J"= 1.5<br>J'= 1 5 | 44197.59<br>2262.57<br>0 228 | 44078.85<br>2268.78<br>0.899 | 44205 54<br>2262 16<br>1 848 | 44064 90<br>2266 35<br>0.977 |
| J"= 2 5<br>J'= 2.5 | 44197 12<br>2262 59<br>1 090 | 44076.50<br>2268.79<br>2.035 | 44209.11<br>2261 98<br>2.451 | 44082.23<br>2268.15<br>2.341 |
| J"= 2.5<br>J = 5 5 | 44187.40<br>2262 58<br>2.143 | 44075.19<br>2262.80<br>2.281 | 44213 30<br>2261.78<br>3 251 | 44092.09<br>2267 98<br>3 603 |
| J"= 4 5<br>J'= 4.5 | 44122 25<br>2262.53<br>3 296 | 44078.62<br>2266.78<br>3.790 | 44218 13<br>2261.52<br>4.013 | 44096 50<br>2227 75<br>4.875 |
| J"= 5 5<br>J'= 5.5 | 44199.74<br>2262 48<br>4.529 | 44077.89<br>2268.73<br>4.546 | 44225.59<br>2261.24<br>4.727 | 44101 44<br>2267 50<br>8.162 |
| J"= 6.5<br>J'= 6.5 | 44201 65<br>2262.55<br>5.628 | 44079 09<br>2266.65<br>5 240 | 44229.88<br>2260.93<br>5 392 | 44106.82<br>2267 22<br>7 531 |
| J"= 7 5<br>J = 7 5 | 44204.60<br>2262 21<br>7 181 | 44081 14<br>2268 54<br>5 877 | 44236 40<br>2260 58<br>6 008 | 44112 94<br>2266.91<br>8 925 |
| J"= 8 5<br>J'= 8 5 | 44207.97<br>2262.04<br>8 591 | 44083 72<br>2268.41<br>5.462 | 44243 75<br>2260.21<br>5.675 | 44119 50<br>2268 57<br>10.368 |
| J"= 8 5<br>J'= 9.5 | 44211 96<br>2261 63<br>10 051 | 44086.84<br>2268.25<br>6.998 | 44251.72<br>2259.20<br>7.092 | 44128.60<br>2268.21<br>11.249 |
| J"=10.5<br>J'=10.5 | 44218 52<br>2261 52<br>11 520 | 44090 51<br>2268.06<br>7.423 | 44260.32<br>2259.36<br>7.575 | 44154.24<br>2265.21<br>13.572 |
| J"=11 5<br>J'=11 5 | 44221.84<br>2261.33<br>13.115 | 44094 72<br>2267.65<br>7 925 | 44269.55<br>2258.89<br>2 008 | 44142.43<br>2265.59<br>14.948 |
| J"=12.5<br>J'=12.5 | 44227.72<br>2261.05<br>14.712 | 44099.47<br>2267.80<br>8 325 | 44279 40<br>2258 39<br>8 400 | 44161.12<br>2264.95<br>12.520 |
| J"=13 5<br>J'=13 5 | 44254.22<br>2260.69<br>16.350 | 44104.77<br>5267.33<br>2.664 | 44289.68<br>2557.85<br>6 753 | 44160.43<br>2264.47<br>16.210 |
| J"=14 5<br>J'=14 5 | 44241 35<br>2260.55<br>18.027 | 44110 82<br>2267.05<br>9.005 | 44300 98<br>2257.29<br>9.089 | 44170 25<br>2263 97<br>19.898 |
| J"=15.5<br>J'=15.5 | 44249 09<br>2259 92<br>19 739 | 44117.01<br>2268.70<br>9.291 | 44312 70<br>2256.69<br>9 551 | 44120 62<br>2263.44<br>21.817 |
| J"=16 5<br>J'=16.5 | 44257 45<br>2258 51<br>21 485 | 44123.85<br>2268.34<br>9 544 | 44325.04<br>2256.08<br>9.599 | 44191 53<br>2262.26<br>23 571 |
| J"=17 5<br>J'=17.5 | 44265 44<br>2259.05<br>23.282 | 44131 43<br>2265 88<br>9.765 | 44338 00<br>2255.40<br>9.818 | 44202.99<br>2262.29<br>25 155 |
| J"=18 5<br>J'=12.5 | 44278.04<br>2258.54<br>25.068 | 44139.47<br>2265.55<br>9.957 | 44351.57<br>2254.71<br>10 005 | 44215 01<br>2261.88<br>28.968 |
| J"=19.5<br>J'=19.5 | 44288 28<br>2258 04<br>28 902 | 44146 06<br>2265 10<br>10.122 | 44365.77<br>2255.99<br>10 168 | 44227.87<br>2261.03<br>28.207 |
| J"=20.5<br>J'=20 5 | 44297.09<br>2257.48<br>28.740 | 44157.20<br>2564.64<br>10.283 | 44380.58<br>2253.24<br>10.305 | 44240.69<br>2250 36<br>30.871 |
| J"=21 5<br>J'=21 5 | 44308.54<br>2256.90<br>30.842 | 44166.90<br>2264.14<br>10.380 | 44388.00<br>2252.45<br>10 420 | 44254.36<br>2259.88<br>32.557 |

V' = 0 V" = 0

Q BRANCH

| | 11 | 12 | 21 | 22 |
|---|---|---|---|---|
| J"=22 5<br>J'=22.5 | 44320.60<br>2258.22<br>52.546 | 44177.15<br>9243.81<br>10.478 | 44412 04<br>2251 64<br>10 513 | 44286.59<br>2259 94<br>34 464 |
| J"=25 5<br>J'=23.5 | 44533.28<br>2255.24<br>54.459 | 44187.98<br>2263 08<br>10 559 | 44428 69<br>2250.20<br>10.587 | 44283 37<br>2258 18<br>36 281 |
| J"=24.5<br>J'=24.5 | 44348.58<br>2254.97<br>32.409 | 44199 32<br>2262 42<br>10.610 | 44445.95<br>2249.92<br>10 844 | 44296.71<br>2257.40<br>32 336 |
| J"=25.5<br>J"=25.5 | 44380.46<br>2254.26<br>38.387 | 44211 24<br>2261.67<br>10.652 | 44463.82<br>2242.02<br>10.684 | 44314.61<br>2256.59<br>40.298 |
| J"=26.5<br>J'=26.5 | 44274.98<br>2253.82<br>40.339 | 44223.73<br>2261.23<br>10.679 | 44422.30<br>2248.08<br>10.709 | 44331.07<br>2255.75<br>42.272 |
| J"=27.5<br>J'=27.5 | 44390.08<br>2252 76<br>42.326 | 44255.77<br>2260.56<br>10.292 | 44501 59<br>2247 12<br>10.721 | 44348.08<br>2254.89<br>44.260 |
| J"=28.5<br>J'=28.5 | 44405.80<br>2251 98<br>44.323 | 44250.37<br>2259.87<br>10.665 | 44521.09<br>2246.15<br>10.721 | 44365.62<br>2254.00<br>48.282 |
| J"=29.5<br>J'=29.5 | 44422.13<br>2251 13<br>46.353 | 44264.53<br>2259.18<br>10.683 | 44541 40<br>2245.10<br>10.709 | 44383.80<br>2253.07<br>48.274 |
| J"=30.5<br>J'=50.5 | 44439.06<br>2250.27<br>48.353 | 44279.26<br>2258 39<br>10.863 | 44562 30<br>2244.05<br>10 566 | 44402.50<br>2252.13<br>50 298 |
| J"=51.5<br>J'=31.5 | 44456 60<br>2249.36<br>50 382 | 44294 55<br>2257 81<br>10.834 | 44585.62<br>2242.97<br>10 658 | 44421 77<br>2251 15<br>52 326 |
| J"=52.5<br>J'=32.5 | 44474.74<br>2248 47<br>52.416 | 44310.41<br>2256.81<br>10.598 | 44605.94<br>2241.65<br>10.619 | 44441.60<br>2250.14<br>54 565 |
| J"=33.5<br>J'=33.5 | 44493.49<br>2247.52<br>54.463 | 44328.83<br>2255.97<br>10.552 | 44628.66<br>2240.71<br>10.573 | 44462.00<br>2249.11<br>56 412 |
| J"=34.5<br>J'=34.5 | 44512.84<br>2246.54<br>56.514 | 44243.82<br>2255.11<br>10.501 | 44651.98<br>2232.54<br>10 521 | 44482.98<br>2248 05<br>58.464 |
| J"=58.5<br>J'=35.8 | 44532.79<br>2245.84<br>58.670 | 44361.37<br>2264.21<br>10 444 | 44675.91<br>5238 54<br>10.464 | 44504.49<br>2246.96<br>60 522 |
| J"=32.5<br>J'=32.5 | 44653.33<br>2244.50<br>60.632 | 44379.49<br>2253.29<br>10.362 | 44700.43<br>2237 11<br>10.401 | 44528.59<br>2245 85<br>62.688 |
| J"=57.5<br>J'=37.6 | 44574.46<br>2243.44<br>62.898 | 44322.18<br>2252.34<br>10.515 | 44725.55<br>2235.28<br>10.334 | 44549 25<br>2244.71<br>64 853 |
| J"=38 5<br>J'=38.5 | 44596.23<br>2242.34<br>64 768 | 44417.44<br>2251.37<br>10.245 | 44751.28<br>2234.57<br>10 282 | 44572.49<br>2243.54<br>68.725 |
| J"=59.5<br>J'=59.5 | 44212.58<br>2241.22<br>66.841 | 44437.27<br>2250.38<br>10.171 | 44777.60<br>2233.26<br>10.188 | 44598 29<br>2242 34<br>68 799 |
| J"=40.5<br>J'=40 5 | 44641.52<br>2240.07<br>68.918 | 44457.87<br>2248.33<br>10 094 | 44204 52<br>2231.92<br>10 111 | 44620.66<br>2241.11<br>70 877 |

# TABLE II-2 (Concluded)

V' = 0 V" = 0

R BRANCH

| | 11 | 12 | 21 | 22 |
|---|---|---|---|---|
| J"= 0.5<br>J'= 1.5 | 44202.60<br>2262.31<br>0 370 | 44082.11<br>2266.49<br>0 000 | 44210.55<br>2351 80<br>0.360 | 44090.05<br>2268.08<br>0.000 |
| J"= 1 5<br>J'= 3 5 | 44205.54<br>2253 15<br>0.950 | 44084.90<br>2255.35<br>0.175 | 44217.42<br>2251.55<br>0.924 | 44096.82<br>2267.74<br>0.201 |
| J"= 2.5<br>J'= 3 5 | 44209.11<br>2251 96<br>1 516 | 44088.23<br>2268.18<br>0 365 | 44225 01<br>2261.12<br>1.392 | 44104 12<br>2367.36<br>0.687 |
| J"= 3 5<br>J'= 4 5 | 44313 30<br>2251.76<br>2 104 | 44092.09<br>2267.98<br>0.950 | 44233.15<br>2260.73<br>1.829 | 44111.97<br>2266 96<br>1 233 |
| J"= 4 5<br>J'= 5.5 | 44216.13<br>2261.52<br>2.713 | 44094.50<br>2267.75<br>1.335 | 44941.22<br>2260.30<br>2.230 | 44120.35<br>2265.53<br>1.830 |
| J"= 3.5<br>J'= 5.5 | 44223.59<br>3361.34<br>3.346 | 44101.44<br>2267.50<br>1.696 | 44251.43<br>2259.81<br>2.602 | 44129.27<br>2266.07<br>2.440 |
| J"= 6 5<br>J'= 7.5 | 44229 66<br>2260.93<br>4.003 | 44105.92<br>2267.22<br>2.033 | 44261.49<br>2259.30<br>3.945 | 44139.73<br>2266.66<br>2.090 |
| J"= 7 5<br>J'= 8.5 | 44236.40<br>2260 55<br>4.665 | 44112.94<br>2266 91<br>2 546 | 44272.16<br>2258.75<br>3.263 | 44148.72<br>2265.07<br>3.786 |
| J"= 8 5<br>J'= 9 3 | 44243.75<br>2260.31<br>5 392 | 44112.50<br>2265.57<br>2.636 | 44283.50<br>3258.18<br>3.555 | 44159.26<br>2364.53<br>4.473 |
| J"= 9.5<br>J'=10.5 | 44251.72<br>2259.60<br>6.131 | 44128 60<br>2236.21<br>2.904 | 44295.45<br>2257 57<br>3.622 | 44170.33<br>2363.96<br>5.203 |
| J"=10.5<br>J'=11.5 | 44260.32<br>2259 36<br>6 873 | 44134.24<br>2255.51<br>2.150 | 44308.03<br>2956.93<br>4.068 | 44181.93<br>2263.37<br>5.957 |
| J"=11.5<br>J'=12.5 | 44269 55<br>2258 69<br>7.646 | 44142.43<br>2255.39<br>3 373 | 44321.23<br>2252.25<br>4 287 | 44124.11<br>2262.74<br>6.734 |
| J"=12.5<br>J'=13.5 | 44279.40<br>2258.39<br>2.440 | 44151.15<br>2364.85<br>3.580 | 44335.06<br>2255.55<br>4.427 | 44206 22<br>2262.09<br>7.533 |
| J"=13.5<br>J'=14.5 | 44289.86<br>2257.85<br>9.253 | 44160.43<br>2364.47<br>3.763 | 44349.52<br>2254.82<br>4.656 | 44220.07<br>2261.42<br>8.351 |
| J"=14.5<br>J'=15.5 | 44300.96<br>2257.29<br>10.086 | 44170 25<br>2253.97<br>3.932 | 44364.59<br>2254 05<br>4.227 | 44933.22<br>2960.71<br>9.190 |
| J"=15.3<br>J'=16.5 | 44312.70<br>2256.69<br>10.834 | 44180 52<br>2253.44<br>4.082 | 44380.29<br>2253.35<br>4.970 | 44246.20<br>2259.92<br>10.046 |
| J"=16.5<br>J'=17.5 | 44325.04<br>2256.06<br>11.900 | 44191.53<br>2262.58<br>4.215 | 44396.50<br>2252.42<br>5 096 | 44263 09<br>2259 23<br>10.919 |
| J"=17.5<br>J'=18.3 | 44338.00<br>2255.40<br>12.681 | 44202.92<br>2262.29<br>4.323 | 44413 54<br>2251.57<br>5.205 | 44278.53<br>2258.43<br>11.808 |
| J"=18.5<br>J'=19 5 | 44351.57<br>2254.71<br>13.576 | 44215.01<br>2261.68<br>4.427 | 44431.09<br>2250.68<br>5.301 | 44294.52<br>2257.62<br>12.712 |
| J"=19.5<br>J'=20.3 | 44365.77<br>2253.99<br>14.485 | 44327.67<br>2261.03<br>4 527 | 44449.25<br>2249.76<br>5.383 | 44311.06<br>2256.77<br>13.530 |
| J"=20.5<br>J'=21.5 | 44380.58<br>2255.24<br>15.405 | 44240.69<br>2260.36<br>4.608 | 44468 04<br>2248.21<br>5.451 | 44328.15<br>2256.60<br>14.361 |
| J"=21.5<br>J'=22.5 | 44396.00<br>2252.45<br>16 352 | 44254.38<br>2259.66<br>4.672 | 44487.44<br>2247.63<br>5.509 | 44345.20<br>2255.00<br>15.503 |

V' = 0 V" = 0

P BRANCH

| | 11 | 12 | 21 | 22 |
|---|---|---|---|---|
| J"=22.6<br>J'=23.5 | 44412.04<br>2351.64<br>17.965 | 44266.59<br>2256.84<br>4.796 | 44507.46<br>2245.81<br>5.555 | 44264.00<br>2254.09<br>12.456 |
| J"=23.5<br>J'=24.5 | 44426.69<br>2250.80<br>18 236 | 44283.37<br>2258.12<br>4.774 | 44528.08<br>2246.77<br>5.591 | 44382.76<br>2253.13<br>17.418 |
| J"=24.5<br>J'=25.5 | 44445.95<br>2249.92<br>19.199 | 44292.71<br>2257.40<br>4.811 | 44549.32<br>2244.70<br>5.818 | 44403.08<br>2252.15<br>18.391 |
| J"=25.5<br>J'=26.5 | 44463.52<br>2249.02<br>20.169 | 44314.51<br>2255.59<br>4.840 | 44571.16<br>2243.60<br>5.638 | 44421.85<br>2231.14<br>19.372 |
| J"=26.6<br>J'=27.5 | 44482.30<br>2248.08<br>21.147 | 44331.07<br>2255.75<br>4.862 | 44593.62<br>2242.47<br>5.649 | 44449.38<br>2250.10<br>20.360 |
| J"=27.5<br>J'=28.5 | 44501.39<br>2247.12<br>22.133 | 44348.08<br>2254.82<br>4.876 | 44616.89<br>2241.21<br>5.654 | 44463.38<br>2242.04<br>21.355 |
| J"=28.5<br>J'=29 5 | 44521.09<br>2242.13<br>23.124 | 44365.66<br>2254.00<br>4.885 | 44640.36<br>2240.15<br>5.652 | 44484.83<br>2247.95<br>23.357 |
| J"=29.5<br>J'=30.5 | 44541.40<br>2245.10<br>24.191 | 44383.50<br>2253.07<br>4.227 | 44664.64<br>2238.91<br>5.645 | 44507.04<br>2242.84<br>23.324 |
| J"=30 5<br>J'=31.5 | 44562.30<br>2244.05<br>25.123 | 44402.50<br>2253.13<br>4.265 | 44682.52<br>3237.56<br>5.632 | 44529.72<br>2245.49<br>24.376 |
| J"=31.5<br>J'=33.5 | 44583.52<br>2242.97<br>26.130 | 44421.77<br>2261.16<br>4.878 | 44715.02<br>2236.39<br>5.815 | 44552.28<br>2244.52<br>25.393 |
| J"=39.5<br>J'=33.5 | 44605.84<br>2241.85<br>27.141 | 44441.60<br>2250.14<br>4.886 | 44741.11<br>2235.08<br>5.994 | 44376.77<br>2343.32<br>28.414 |
| J"=55.5<br>J'=34.5 | 44622.62<br>3240 71<br>28.156 | 44469.00<br>2248.11<br>4.851 | 44767.20<br>2233.75<br>5.569 | 44601.14<br>2242.09<br>27.439 |
| J"=34.5<br>J'=35.5 | 44651.96<br>2939.54<br>29.176 | 44482.96<br>9248.05<br>4.833 | 44785.10<br>2232.39<br>5.540 | 44626.08<br>2240.34<br>28.467 |
| J"=35.5<br>J'=36.5 | 44675 91<br>2238.34<br>30.195 | 44504.49<br>2246.96<br>4.811 | 44823.00<br>2231.00<br>5.509 | 44631.39<br>2239.56<br>29.498 |
| J"=36.5<br>J'=37.5 | 44700.43<br>2337.11<br>31.220 | 44526.59<br>2345.85<br>4.787 | 44251.50<br>2229.58<br>5.472 | 44677.46<br>2238.23<br>20.631 |
| J"=37.5<br>J'=38.5 | 44725.55<br>2335.86<br>32.246 | 44549.25<br>2944.71<br>4.760 | 44880.50<br>2228.13<br>3.440 | 44704.30<br>2236.92<br>31.667 |
| J"=38.5<br>J'=39.5 | 44751.28<br>2234.57<br>33.275 | 44572.49<br>2242.54<br>4.731 | 44910.30<br>2226.66<br>6.402 | 44731.51<br>2235.56<br>32.605 |
| J"=39.3<br>J'=40.3 | 44777.60<br>2233.25<br>34.305 | 44598.29<br>2242.34<br>4.701 | 44840.60<br>2223.12<br>3.362 | 44759.29<br>2234.17<br>33.644 |

UNCLASSIFIED

Security Classification

**DOCUMENT CONTROL DATA - R & D**

*(Security classification of title, body of abstract and indexing annotation must be entered when the overall report is classified)*

| | |
|---|---|
| 1 ORIGINATING ACTIVITY *(Corporate author)*<br>Arnold Engineering Development Center<br>Arnold Air Force Station, Tennessee 37389 | 2a. REPORT SECURITY CLASSIFICATION<br>UNCLASSIFIED<br>2b. GROUP N/A |

3 REPORT TITLE

RESONANCE LINE ABSORPTION METHOD FOR DETERMINATION OF NITRIC OXIDE CONCENTRATION

4 DESCRIPTIVE NOTES *(Type of report and inclusive dates)*

Final Report

5 AUTHOR(S) *(First name, middle initial, last name)*

W. K. McGregor and J. D. Few, ARO, Inc., and C. D. Litton, UTSI

| | | |
|---|---|---|
| 6 REPORT DATE<br>December 1973 | 7a. TOTAL NO OF PAGES<br>64 | 7b NO OF REFS<br>19 |
| 8a CONTRACT OR GRANT NO<br>b. PROJECT NO<br>c. Program Element 65802F<br>d. | 9a. ORIGINATOR'S REPORT NUMBER(S)<br>AEDC-TR-73-182<br>9b OTHER REPORT NO(S) *(Any other numbers that may be assigned this report)*<br>ARO-ETF-TR-73-113 | |

10 DISTRIBUTION STATEMENT

Approved for public release; distribution unlimited.

| | |
|---|---|
| 11 SUPPLEMENTARY NOTES<br>Available in DDC. | 12 SPONSORING MILITARY ACTIVITY<br>Arnold Engineering Development Center, Arnold Air Force Station, Tennessee 37389 |

13. ABSTRACT The details of the derivation of working equations for the determination of the concentration of nitric oxide for measurement of the absorption of individual spectral lines lying between 2270 and 2260 Å in the NO (0,0) γ-band are presented. It is shown experimentally that the derivation is accurate, that published values of oscillator strengths are adequate, and that measurements of number densities with uncertainty no greater than ±20 percent are possible when proper corrections for the relative line widths of source and absorber are made. The density range of use of the (0,0) γ-band is from about $10^{14}$ to $10^{16}$ $cm^{-3}$ for path lengths usually encountered in combustion system testing (10 to 100 cm). Extension of the range to larger concentrations by use of the (0,1) γ-band and the application to media having non-uniform concentration and temperature are discussed.

DD FORM 1 NOV 65 1473

UNCLASSIFIED

Security Classification

UNCLASSIFIED

Security Classification

| 14. KEY WORDS | LINK A ROLE | LINK A WT | LINK B ROLE | LINK B WT | LINK C ROLE | LINK C WT |
|---|---|---|---|---|---|---|
| absorption spectra | | | | | | |
| band spectra | | | | | | |
| combustion efficiency | | | | | | |
| concentration | | | | | | |
| nitrogen oxide | | | | | | |

AFSC
Arnold AFS Tenn

UNCLASSIFIED

Security Classification